



Olive leaf extract impairs mitochondria by pro-oxidant activity in MDA-MB-231 and OVCAR-3 cancer cells

Reyes Benot-Dominguez^{a,1}, Maria Grazia Tupone^{a,b,1}, Vanessa Castelli^a, Michele d'Angelo^a, Elisabetta Benedetti^a, Massimiliano Quintiliani^{a,c}, Benedetta Cinque^a, Iris Maria Forte^d, Maria Grazia Cifone^a, Rodolfo Ippoliti^a, Barbara Barboni^e, Antonio Giordano^f, Annamaria Cimini^{a,f,*}

^a Department of Life, Health and Environmental Sciences, University of L'Aquila, 67100, L'Aquila, Italy

^b Center for Microscopy, University of L'Aquila, 67100, L'Aquila, Italy

^c S.I.R.E. srl, 80129, Napoli, Italy

^d Cell Biology and Biotherapy Unit, Istituto Nazionale Tumori-IRCCS-Fondazione G. Pascale, I-80131, Napoli, Italy

^e Faculty of Bioscience and Technology for Food, Agriculture and Environment, University of Teramo, 64100, Teramo, Italy

^f Sbarro Institute for Cancer Research and Molecular Medicine and Center for Biotechnology, Temple University, Philadelphia, PA, 19122, USA

ARTICLE INFO

Keywords:

OLE
Mediterranean diet
TNBC
Ovarian cancer
Mitochondria
ROS

ABSTRACT

Breast and ovarian cancers are the leading and fifth reason for tumor death among females, respectively. Recently, many studies demonstrated antiproliferative activities of natural alimments in cancer. In this study, we investigated the antitumor potential of Olive Leaf Extract (OLE) in triple-negative breast and ovarian cancer cells.

A HPLC/DAD analysis on OLE has been performed to assess the total polyphenolics and other secondary metabolites content. HCEpiC, MDA-MB-231, and OVCAR-3 cell lines were used. MTS, Cytofluorimetric, Western Blot analysis were performed to analyze cell viability, cell proliferation, apoptosis, and oxidative stress. Fluorimetric and IncuCyte® analyses were carried out to evaluate apoptosis and mitochondrial function.

We confirmed that OLE, containing a quantity of oleuropein of 87 % of the total extract, shows anti-proliferative and pro-apoptotic activity on MDA-MB-231 cells. For the first time, our results indicate that OLE inhibits OVCAR-3 cell viability inducing cell cycle arrest, and it also increases apoptotic cell death up-regulating the protein level of cleaved-PARP and caspase 9. Moreover, our data show that OLE treatment causes a significant decrease in mitochondrial functionality, paralleled by a reduction of mitochondrial membrane potential. Interestingly, OLE increased the level of intracellular and mitochondrial reactive oxygen species (ROS) together with a decreased activity of ROS scavenging enzymes, confirming oxidative stress in both models. Our data demonstrate that mitochondrial ROS generation represented the primary mechanism of OLE antitumor activity, as pretreatment with antioxidant N-acetylcysteine prevented OLE-induced cell cycle arrest and apoptosis.

1. Introduction

Breast cancer is the most frequently diagnosed cancer in women

worldwide (254 % of the total) and the main cause of tumor death among females (15 %), according to the WHO 2018 cancer statistics.

Ovarian cancer, instead, is the fifth most common reason for tumor

Abbreviations: DCF, 2', 7'- dichlorofluorescein; DCFDA, 2', 7'- dichlorofluorescein diacetate; DNP, 2, 4-dinitrophenylhydrazone; HCEpiC, Human Corneal Epithelial Cells; HGSO, High-Grade Serous Ovarian Carcinoma; NAC, N-acetylcysteine; OLE, Olive leaf extract; PVDF, polyvinylidene difluoride; ROS, reactive oxygen species; TMRM, tetramethylrhodamine methyl ester perchlorate; TNBC, triple negative breast cancer.

* Corresponding author at: Department of Life, Health and Environmental Sciences, University of L'Aquila, 67100, L'Aquila, Italy.

E-mail addresses: rdominguezbenot@unite.it (R. Benot-Dominguez), maria Grazia.tupone@univaq.it (M.G. Tupone), vanessa.castelli@univaq.it (V. Castelli), michele.dangelo@univaq.it (M. d'Angelo), elisabetta.benedetti@univaq.it (E. Benedetti), mquintiliani@unite.it (M. Quintiliani), benedetta.cinque@univaq.it (B. Cinque), m.forte@istitutotumori.na.it (I.M. Forte), maria Grazia.cifone@univaq.it (M.G. Cifone), rodolfo.ippoliti@univaq.it (R. Ippoliti), bbarboni@unite.it (B. Barboni), giordano@temple.edu (A. Giordano), annamaria.cimini@univaq.it (A. Cimini).

¹ These authors contributed equally to this work.

<https://doi.org/10.1016/j.bioph.2020.111139>

Received 9 September 2020; Received in revised form 10 December 2020; Accepted 10 December 2020

Available online 24 December 2020

0753-3322/© 2020 The Authors.

Published by Elsevier Masson SAS. This is an open access article under the CC BY-NC-ND license

(<http://creativecommons.org/licenses/by-nc-nd/4.0/>).

failure in women and the leading cancer-causing mortality from gynecological malignancy in the developed world [1,2]. Due to their aggressiveness and difficulty of diagnosis in the early stages, prevention through a correct lifestyle is considered a concrete strategy. In this context, diet and nutraceutical supplements become important either as prevention that favors a prognostic approach or a way to increase the survival rates as well. Therefore, the identification of new therapeutic strategies focused on inhibiting cancer cell proliferation and inducing apoptosis has become, nowadays, a major dare. In the last decades, the study of the antitumor properties of food components is gaining more and more attention. Recently, scientists from all around the world are focusing their attention on the engaging link between the Mediterranean Diet and its benefits in terms of health, longevity, and quality of life. Indeed, several pieces of research have already demonstrated the anti-proliferative and antiangiogenic activities of natural aliments such as mangosteen, grape, tomato, or chestnut extracts. Modifications in diet habits and adherence to the Mediterranean diet can importantly increase life expectancy, reduce the risk of developing cancer or chronic diseases, and improve the overall well-being [3,4]. Hence, any advance in the comprehension of how dietary-based strategies may affect the biomolecular pathways activated in cancer is strongly needed. Multiple lines of evidence suggest the essential and fundamental role of diet in the prevention and recurrence of the breast [5,6] and ovarian carcinoma [7–9]. More precisely, antioxidants are recently gaining importance in the field of cancer, as its assumption has shown a reduced tumor recurrence and related mortality in breast cancer patients [10]. Historically, among natural foods, *Olea europaea* leaf extracts were extensively used as a cure for fever and other disorders such as malaria [11]. Over the years, olive phenolic compounds, which are large in number in olive leaves, have shown great interest and have been studied for their potential health benefits. *Olea europaea* leaf extracts, hereafter abbreviated as OLE, have shown a remarkable anti-tumor [12], anti-inflammatory [13], anti-viral [14], antithrombotic [15], anti-microbial [16], hypocholesterolemic [17], skin photoprotective properties [18], anti-proliferative and pro-apoptotic effect in several cancer cell lines such as MDA-MB-231 [19–21], SkBr3 [22], MCF-7 [22,23], JIMT-1 [24], Caco-2 [25], A375 [26] and HeLa cells [27]. Indeed, polyphenols have been reported to interfere with the initiation, promotion, and progression phases of cancer by affecting tumorigenic cell transformation [28,29]. In fact, olive oil-based diets showed a significant reduction of induced pre-cancerous breast lesions in vivo, and a protective role against mammary cancer development in perinatal exposed female offspring [30], interacting with conventional anti-tumor therapies [31,32]. OLE contains higher amounts and variety of polyphenols than those found in extra virgin oil, and OLE polyphenols present structural differences that may be responsible for better bioavailability, as extensively reviewed by Boss and colleagues [33]. In addition, it has been published that Oleuropein, the main polyphenol of *Olea europaea* leaf extract, was more efficient to enhance the cytotoxic activity in co-administration with conventional chemotherapeutic approaches, respect to Oleuropein alone [34]. To understand the potential biological effects of phenolic compounds, several scientists were also concentrated upon essential characteristics such as bioavailability and metabolism [35,36]. Polyphenols can act as inhibitors of tumor cell proliferation, thanks to their capability to control the activity and the expression of many target genes implicated in tumorigenesis while influencing only slightly normal cells [37]. Natural polyphenols have been demonstrated to exert beneficial and protective effects due to their antioxidant ability as scavengers of free radical produced from many cellular processes and various other sources into the environment [38]. However, recently many pieces of evidence suggest a pro-oxidant response exerted by polyphenols through the modulation of chemical signaling pathways inducing anti-proliferative and pro-apoptotic responses in pre-tumoral and tumoral cells [39–41]. The Reactive Oxygen Species (ROS) play a leading role in tumorigenesis [42], supporting the antitumor activity of different anti-cancer drugs. In this regard, pro-oxidant compounds could

have a cytotoxic action, producing increased levels of ROS in cancer cells, leading to an increased oxidative stress and damaging different human tissues [43]. There is an increasing interest on investigating the pathways that regulate ROS production, as well as their effects on various aspects of mitochondrial biogenesis, fatty acid oxidation and redox homeostasis, considering that polyphenols-induced ROS increase could represent an efficient approach to selectively destroy tumoral cells [43]. Nevertheless, Olive leaves still remain a non-edible source rich in polyphenols that can perform a very interesting role in cancer, contributing to block tumor progression as already reported [26]. Several studies have investigated on the bioactive elements present in OLE and indicated the biophenols oleuropein and hydroxytyrosol as the main components responsible for the observed effects [44]. Breast and ovarian cancer continue to be major health threats for women. Breast cancer is the most frequently occurring cancer in women, and an increased familial risk of breast cancer is associated with an increased risk of ovarian cancer [45,46]. In the present study, we analyzed the antitumoral impact of OLE on human triple negative breast (TNBC) cell line, MDA-MB-231, and on High-Grade Serous Ovarian Carcinoma (HGSO) cell line, OVCAR-3. TNBC constitutes a highly varied and malignant breast cancer subtype where none of the three receptors are expressed (estrogen, progesterone, nor HER-2/neu) and, consequently, impede these patients to respond to any hormonal nor targeted therapy. Moreover, only standard chemotherapy has been officially approved for its routine treatment, as the absence of clear tumor drivers hinders the reaching of better therapeutic achievements. OVCAR-3 is one of the most extensively cell line used as a HGSO model for drug resistance in ovarian cancer, due to its low effectiveness to cyclophosphamide, cisplatin and doxorubicin. Besides, even if ovarian tumor is significantly less frequent than breast cancer, it comparatively develops in a much more aggressive profile. Considering all types of ovarian cancers, the 5-year survivors neither reach 50 % of the total. It means 5% of overall demises in females, making it the deadliest gynecological cancer, with only a few effective treatment options available. In this work, we provided evidence that OLE induced cell cycle arrest, apoptosis and death through ROS generation. We also proved that OLE specifically operated as toxic pro-oxidant compound on MDA-MB-231 and OVCAR-3 cell lines. To the best of our knowledge, this is the first investigation on the antitumor effect of OLE related to its pro-oxidant activity in MDA-MB-231 and OVCAR-3 cells, specifically focalizing interest in the effects exerted in both models on mitochondrial functionality and cellular redox homeostasis.

2. Materials and methods

2.1. Reagents and cells

Olive leaf extract (OLE) was provided and characterized (Supplementary File 1) by Oleafit S.R.L. (Isola del Gran Sasso D'Italia, TE, Italy), and OLE working solution was prepared fresh at a final concentration of 200 µg/mL for HCEpiC, MDA-MB-231, MDA-MB-468, OVCAR-3, and OVCAR-8 cells, by suspending the powder extract in the appropriate volume of complete cell culture media. Human corneal epithelial primary cells HCEpiC were isolated from the healthy human cornea and were provided by Innoprot (P10871; RRID: CVCL_1272; Innoprot, Bizkaia, Spain). HCEpiC cells were used as a model of healthy normal epithelial cells as an internal control. MDA-MB-231 (ECACC 92,020,424; RRID: CVCL_0062) and OVCAR-3 (ATCC® HTB-161™; RRID: CVCL_0465) were purchased from ECACC® (Porton Down, England) and ATCC® (Manassas, VA, USA), respectively. MDA-MB-468 cells (ATCC® HTB-132; RRID: CVCL_0419) represent an additional TNBC cancer cell model of *in vitro* studies. OVCAR-8 cells, one of the most resistant ovarian cancer lines to cisplatin chemotherapy, were originally acquired from ATCC (RRID: CVCL_1629). Experiments were carried out at passage numbers 5–8 for HCEpiC, at 52–54 for MDA-MB-231 cells, and between 7–12 for OVCAR-3, OVCAR-8, and MDA-MB-468 cells. For

all the experiments, HCEpiC cells were grown in complete IM-Corneal Epithelial Cell Medium (CEpiCM) (P60131; Innoprot, Bizkaia, Spain), MDA-MB-231 were cultured in Dulbecco's modified Eagle's medium-high glucose (DMEM), while MDA-MB-468 cells were maintained in DMEM/DMEM F12 (1:1). RPMI 1640 was the culture medium employed for OVCAR-3 and OVCAR-8 cells, with 10 % Heat-inactivated fetal bovine serum, 1% Penicillin-Streptomycin and 1% L-Glutamine (all of them from Corning Life Sciences, Corning, NY, USA) and 0.01 mg/mL Bovine Insulin was also supplemented for OVCAR-3 medium (Sigma-Aldrich, St. Louis, MO, USA). Cells were detached once they reached 70–80 % of confluence by using 0.25 % Trypsin-EDTA (25–052-CI, Corning Life Sciences, NY, USA) and seeded onto a culture dish, flask, or 96-Multiwell plate at 10,000 cells/cm² (HCEpiC and MDA-MB-231) or 25,000 cells/cm² (OVCAR-3). Cells were maintained in a 5% CO₂ humidified atmosphere at 37 °C.

2.2. MTS cell viability colorimetric assay

For testing the effect of OLE and oleuropein on cell viability, cells were plated into 96-well microplates at a density of 5000 cells/cm² for MDA-MB-468, 10,000 cells/cm² for HCEpiC and MDA-MB-231 or 25,000 cells/cm² for OVCAR-3 and OVCAR-8. The day after, cells were treated for 24 and 72 h with the indicated concentrations of OLE and oleuropein spanning a range to 0–400 µg/mL for OLE, to 0–400 µM for oleuropein. MTS Cell Proliferation analysis, CellTiter® AQueous One Solution Cell Proliferation Assay (Promega Corporation Madison, WI, USA) was used, in accordance with the supplier's guidelines. The indication of viability, determined by the amount of formazan produced, was analyzed by an ELISA Infinite F200 plate reader (Tecan, Swiss). The analysis was carried out at least in triplicates. The results were read as absorbance at 492 nm. The same procedure was used to evaluate the effect of NAC on cell viability in cells treated with OLE, with or without 5 mM NAC pretreatment.

2.3. Clonogenic assay

For colony formation assay, 500 cells/well were seeded into 6-well plates and allowed to attach overnight. The day after, the culture medium was replaced with a fresh one, containing serial dilutions of OLE for 24 h at the three following concentrations: 25 µg/mL, 50 µg/mL, and 100 µg/mL or culture medium, used as a control. Once the 24 h of treatment were completed, the respective medium containing OLE was changed to avoid excessive cell death in the very sparse cell cultures, which were incubated until colonies were formed. Approximately 7–10 days after, colonies were subsequently washed with PBS, fixed with methanol, and stained at room temperature for 30 min with crystal violet solution (Cat. no. HT90132; Sigma Aldrich, Saint Louis, MO, USA) and additionally washed with PBS.

2.4. Cell cycle profile analysis by flow cytometer

The cell cycle profile experiment was analyzed by propidium iodide (PI) cell DNA staining. MDA-MB-231, MDA-MB-468, OVCAR-3, and OVCAR-8 cells, untreated and treated with OLE at 200 µg/mL for 24 h, were subjected to enzyme separation by using Accutase™ solution (37 °C, 10 min) from PAA-GE Healthcare Life Sciences (GE Healthcare Bio-Sciences AB, SE-751 84 Uppsala Sweden) and next centrifuged (1.200 rpm, 10 min, 4 °C). The obtained pellets were ice-cold PBS washed and fixed in 70 % ice-cold ethanol (4 °C, 30 min). The fixed cells were placed into plastic BD tubes (Becton Dickinson, San José, CA, USA), washed two times with ice-cold PBS, and dyed with a combination of PI (50 µg/mL), Nonidet-P40 (0.1 % v/v), and RNase A (6 µg/10⁶ cells) solution (Sigma-Aldrich, Saint Louis, MO, USA) for 1 h at 4 °C in the dark. The subdivision of cell cycle phases was investigated by using a flow cytometer. Data from 10,000 events per sample were collected and analyzed using FACSCalibur Flow Cytometry System (RRID:

SCR_000401; Beckton Dickinson, San Jose, CA, USA) instrument equipped with cell cycle analysis software (Modfit LT for Mac V3.0).

2.5. Western blotting analysis

Both treated and untreated cells were scratched and lysed as previously described, and the total concentration of protein was assessed [47, 48]. Control and treated cell resulting lysates (20–50 µg of proteins/sample) were loaded on 8–13 % polyacrylamide SDS denaturing gels (BIO-RAD, CA, USA). The lysates were separated and then transferred to polyvinylidene difluoride (PVDF) membranes, as previously described [47,48]. Unspecific binding sites were blocked with 5% (w/v) non-fat dry milk (Bio-Rad Laboratories, Hercules, CA) dissolved in Tris-buffer saline containing 0.1 % (v/v) Tween20 (TBS-T). Membranes were maintained at 4 °C overnight with the following primary antibodies diluted in blocking solution: Cyclin B2/CCNB2 1:200 (Abcam, Cat# ab18250; RRID: AB_444357), anti-Cyclin D1 1:10000 (Abcam Cat# ab134175, RRID:AB_2750906), anti-cleaved Caspase-9 1:1000 (Cell Signaling Technology Cat# 9509, RRID:AB_2073476); anti-caspase-8 p18 1:200 (Santa Cruz Biotechnology Cat# sc-7890, RRID:AB_2068330); anti-cleaved PARP 1:1000 (Thermo Fisher Scientific Cat# 44–698 G, RRID:AB_2533726), anti-Catalase 1:200 (Rockland Cat# 200–4151, RRID:AB_2071858), and anti-Mn SOD 2 1:2000 (Enzo Life Sciences Cat# SOD-111D, RRID:AB_2302158) and β-Actin (8H10D10, RRID:AB_10694076) Mouse mAb (HRP Conjugate) (Cell Signaling Technology Cat#12,262). Subsequently, membranes were three times-washed with TBS-T and following incubated with the secondary HRP conjugated anti-mouse or anti-rabbit IgG antibody, diluted 1:30,000 in blocking solution for 1 h at Room Temperature with soft agitation. After washing the membranes four times with TBS-T, immunoreactive bands were observed by ECL, by following the supplier's guidelines. Alliance 4.7 UVITEC (Cambridge, UK) was employed to obtain the individual bands from whole cell lysate, which were later analyzed by ImageJ software and normalized to β-actin. Values were expressed as relative units (R.U.).

2.6. Annexin V apoptosis assay by IncuCyte® S3 live-cell analysis system

IncuCyte® S3 Live-Cell Analysis System (Sartorius, Michigan, MI, USA) was employed to assess the apoptotic effect of OLE on HCEpiC, MDA-MB-231, and OVCAR-3 cells. This analytical instrument enables an automatic in-incubator way to monitor live cells. Briefly, cells were plated in a 96-multiwell culture plate at 10,000 cells/cm² (HCEpiC, MDA-MB-231) and 25,000 cells/cm² (OVCAR-3), and maintained for 24 h at 37 °C before applying the OLE treatment at a concentration of 200 µg/mL. Early apoptotic cells were observed by IncuCyte® Annexin V Green Reagent staining, which was diluted in complete medium to yield a final dilution of 1:200. Cell nuclei were detected by IncuCyte® NuLight Red reagent without affecting cell growth or morphology, at a final dilution of 1:2000. Cell images were captured using phase contrast, green (300 ms exposure), and red (400 ms exposure) channels in the IncuCyte ZOOM™ platform (Essen BioScience, Inc.), which is positioned into a cell incubator at 37 °C and 5% CO₂. An amount of four picture sets was taken from several points of the well, using a 10x dry objective lens every 4 h for a total timeline of 72 h, and all the treatment conditions were run in quadruplicates. Automated real-time evaluation using live-cell analysis (Essen Bioscience) was carried out by assessing as green area for all cells stained with Annexin V Reagent, and normalizing them to the red area, established for all cells stained red with NuLight Reagent. Graphics were made using the basic software graph tools (Essen Bioscience).

2.7. OxyBlot™ analysis

OxyBlot analysis was carried out by following strictly the protocol's instructions provided by the manufacturer (Millipore, Billerica, MA) to

characterize the carbonyl groups inserted in the amino acid side chain, following the change in the oxidative state of proteins. The grade of protein oxidation was identified by an Oxidized Protein Detection Kit (OxyBlot, Chemicon Cat# S7150-Kit). This kit generates 2, 4-dinitrophenylhydrazone (DNP) moiety from carbonyl groups. The DNP moiety can be later individuated with anti-DNP antibodies, a technique to test for one form of oxidative damage to a protein. The proteins were derivatized following the protocol's instructions. The protein lysates were isolated on 10 % SDS-PAGE gels and electroblotted onto PVDF membranes. Consequently, membranes were blocked by using 5% milk (in Tris Buffered Saline [TBS] with 0.2 % Tween-20) (1 h, room temperature). The PVDF membranes were incubated with a primary rabbit anti-DNP protein antibody from Chemicon Oxyblot (working dilution, 1:150) overnight at 4 °C, and to a secondary antibody afterward [Goat Anti-Rabbit IgG (HRP conjugated)] (working solution, 1:300; 1 h, room temperature). Next, washing buffer TBS with 0.2 % Tween-20 was used to perform three washes of the membranes. The protein bands were then observed with ECL (Amersham Biosciences), while band signal intensity was analyzed by means of a flatbed scanner (Epson Perfection 3200 PHOTO) and imaging software (Image J).

2.8. Oxidative stress and reactive oxygen species by fluorimetric assay

To study whether OLE was able to induce oxidative stress, ROS production was investigated in MDA-MB-231 and OVCAR-3 cells by using DCFDA Cellular ROS Detection Kit (Abcam). The assay is performed using the fluorogenic agent 2',7'- dichlorofluorescein diacetate (DCFDA), which is able to diffuse into the cells and be deacetylated by cellular esterases to a nonfluorescent compound, following later oxidation by ROS to 2', 7'- dichlorofluorescein (DCF). For this purpose, both MDA-MB-231 and OVCAR-3 cells were plated into 96-multiwell plates at cell densities of 25,000 cells/well. Twenty-four hours later, the cells were washed with PBS and incubated with 10 μ M DCFDA diluted in phenol red-free medium (DMEM F12, Corning) for 40 min at 37 °C in the dark, according to the provider's instructions. After an additional wash with PBS, cells were then incubated with or without 200 μ g/mL OLE using their specific medium. After 24 h, fluorescence was evaluated at excitation of 495 nm and emission of 529 nm using a Victor3 microplate reader (PerkinElmer, Waltham, MA, USA). For data analysis, blank readings were subtracted to every single measurement in order to determine the fold change from assay (control and treated), and data were normalized to $t = 0$.

2.9. Determination of N-acetyl cysteine effects on OLE-induced cell viability, apoptosis, and mitochondrial impairment

Treatment with N-acetyl cysteine (NAC) has been used because of its specific activity as a ROS scavenger. HCEpiC, a model of healthy normal epithelial cells used as internal control, MDA-MB-231, and OVCAR-3 tumor cells, were seeded at their specific cell densities. After 24 h, cells were subjected to pretreatment with 5 mM NAC for 1 h. Subsequently, they were incubated with 200 μ g/mL OLE for 24 h, and cell viability, apoptosis, and mitochondrial ROS measurement were determined as described.

2.10. Analysis of mitochondrial function by fluorimetric assay and mitochondrial membrane potential by fluorimetric assay and by IncuCyte® S3 live-cell analysis system

For elucidating the presence of alterations in mitochondrial functions, fluorescence analysis was carried out with MitoTracker® Green FM probe (Invitrogen). MDA-MB-231 and OVCAR-3 cells, after treatment with 200 μ g/mL OLE for 24 h, were incubated for 30 min at 37 °C with 200 nM MitoTracker® Green FM probe. Culture media were then replaced with PBS in order to avoid phenol red interferences. Fluorescence was immediately measured using a Victor3 microplate reader

(PerkinElmer, Waltham, MA, USA).

Changes in mitochondrial membrane potential ($\Delta\Psi_m$) were recorded with tetramethylrhodamine methyl ester perchlorate (Image-iT™ TMRM, Invitrogen). TMRM is a red-fluorescing, cationic and cell-permeant dye, confined by active mitochondria, indicating mitochondrial polarization. MDA-MB-231 and OVCAR-3 cells were loaded with 100 nM TMRM for 30 min at RT. Culture media were then replaced with PBS in order to avoid phenol red interferences, and fluorescence was immediately measured in a Victor3 microplate reader (PerkinElmer, Waltham, MA, USA). In order to corroborate previous results, additional fluorescent analysis with TMRM was carried out in a 96-multiwell plate (Corning Life Sciences, NY, USA) by using IncuCyte® S3 Live-Cell Analysis System (Essen BioScience, Inc.). After washing with complete fresh media, fluorescence was measured on the IncuCyte® S3 Live-Cell Analysis System (Essen BioScience, Inc.). Images were taken using phase contrast with the red channel (exposure: 400 ms) by the IncuCyte ZOOM™ platform (Essen BioScience, Inc.). From different regions, four image sets per well were taken, using a 10x dry objective lens, every 4 h for a total of 72 h, running each condition in quadruplicates. The live-cell analysis of the automated real-time experiment was evaluated as a red area for cells stained with TMRM normalized on the contrast phase area. The basic graph software was used to create final graphics (Essen Bioscience).

2.11. Mitochondrial superoxide assay by IncuCyte® S3 live-cell analysis system

Superoxide produced by mitochondria was evaluated by staining the cells with the Mitochondrial Superoxide Indicator MitoSOX™ Red, used for experiments in live-cell imaging. The MitoSOX™ Red reagent fluorogenic probe selectively binds the mitochondria in live cells. The Oxidation process of MitoSOX™ Red reagent generates red fluorescence. MitoSOX™ Red reagent spread throughout live cells, specifically targeting mitochondria. It is then oxidized quickly by superoxide, and the oxidized compound is highly fluorescent upon binding to the nucleic acid. In order to perform this analysis, HCEpiC, MDA-MB-231, and OVCAR-3 cells were plated into 96-multiwell plates at their cell densities. After 24 h, cells were treated with or without 200 μ g/mL of OLE in their specific media. Twenty-four hours later, cells were incubated with 5 μ M MitoSOX™ Red diluted in Hank's Balanced Salt Solution/Ca/Mg (HBSS, Thermo Fisher Scientific, Grand Island, N.Y., USA) for 30 min at 37 °C, following a PBS washing and then imaged immediately. The level of mitochondria-specific reactive oxygen species (ROS) was monitored up to 6 h and quantified with the oxygen radical-sensitive probe-MitoSOX, by using the IncuCyte live-cell Imaging System. Four images were taken per well, and the mean intensity of fluorescence of MitoSOX™ Red was evaluated for every single image utilizing IncuCyte ZOOM software and then mediated for each well.

2.12. Statistical analysis

The results are presented as mean \pm SEM of triplicate observations from one representative of at least three experiments with similar results. Data were mediated, and statistical analyses were carried out. Samples' statistical analyses were evaluated by Graph Pad Prism 8 software (RRID: SCR_002798) by applying the unpaired Student's *t*-test, and the significance of differences between groups was determined by two-way analysis of variance (ANOVA) followed by Tukey post hoc tests for multiple comparisons. Every single experiment was replicated at least thrice ($n = 3$). Statistically significance was settled at *, $p < 0.05$; **, $p < 0.005$; ***, $p < 0.0001$. Data were presented as mean \pm SEM of three single experiments ($n = 3$).

3. Theory

Breast and ovarian cancer are two of the most common and

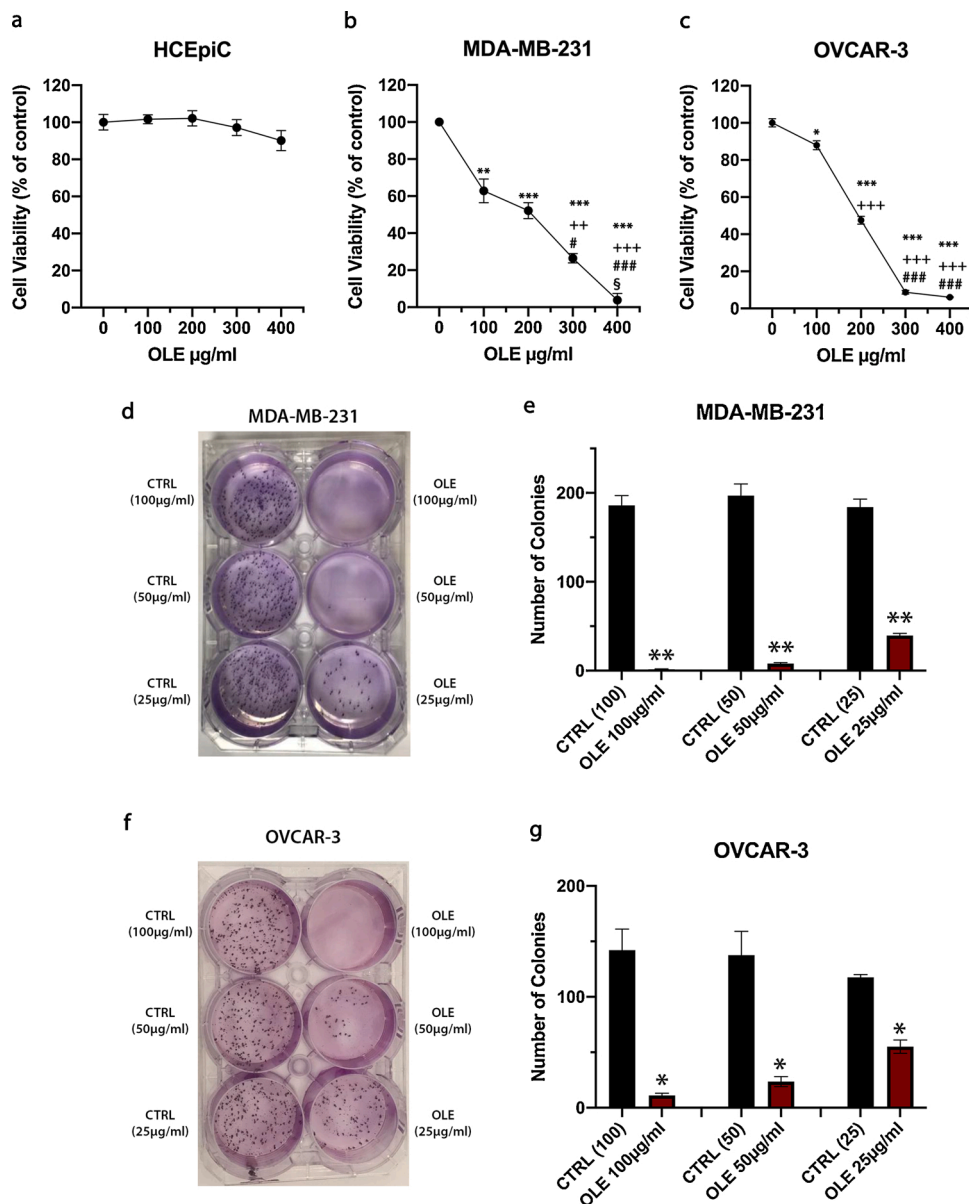


Fig. 1. OLE inhibits specifically MDA-MB-231 and OVCAR-3 cell viability, without affecting non-tumoral cells. Short-term effect of OLE on HCEpiC (a), MDA-MB-231 (b), and OVCAR-3 (c) cell viability. HCEpiC, MDA-MB-231, and OVCAR-3 cells were maintained for 24 h in supplemented or not (control) medium with OLE at the concentrations indicated in the figure. Then, cell viability was evaluated by MTS experiment and presented as a percent of non-treated cells. Long-term Colony formation assay in MDA-MB-231 (d-e) and OVCAR-3 (f-g) cells. (d,f) Representative images of colony formation assay in MDA-MB-231 (d) and in OVCAR-3 (f) cells. (e,g) Graphical representation of the number of treated colonies (red bars) relative to colony count of untreated cells (black bars) in MDA-MB-231 (d) and OVCAR-3 (f) plates. Statistical analysis was carried out by applying the unpaired Student's *t*-test and the one-way analysis of variance (ANOVA) followed by Tukey post hoc tests for multiple comparisons. Statistically significance was settled at * $p < 0.05$, ** $p < 0.005$ vs 0; ++ $p < 0.005$, +++ $p < 0.0001$ vs 100; # $p < 0.05$, ### $p < 0.0001$ vs 200; § $p < 0.05$ vs 300. Data are presented as mean \pm SEM of three different experiments; (n = 3). (For interpretation of the references to colour in the Figure, the reader is referred to the web version of this article).

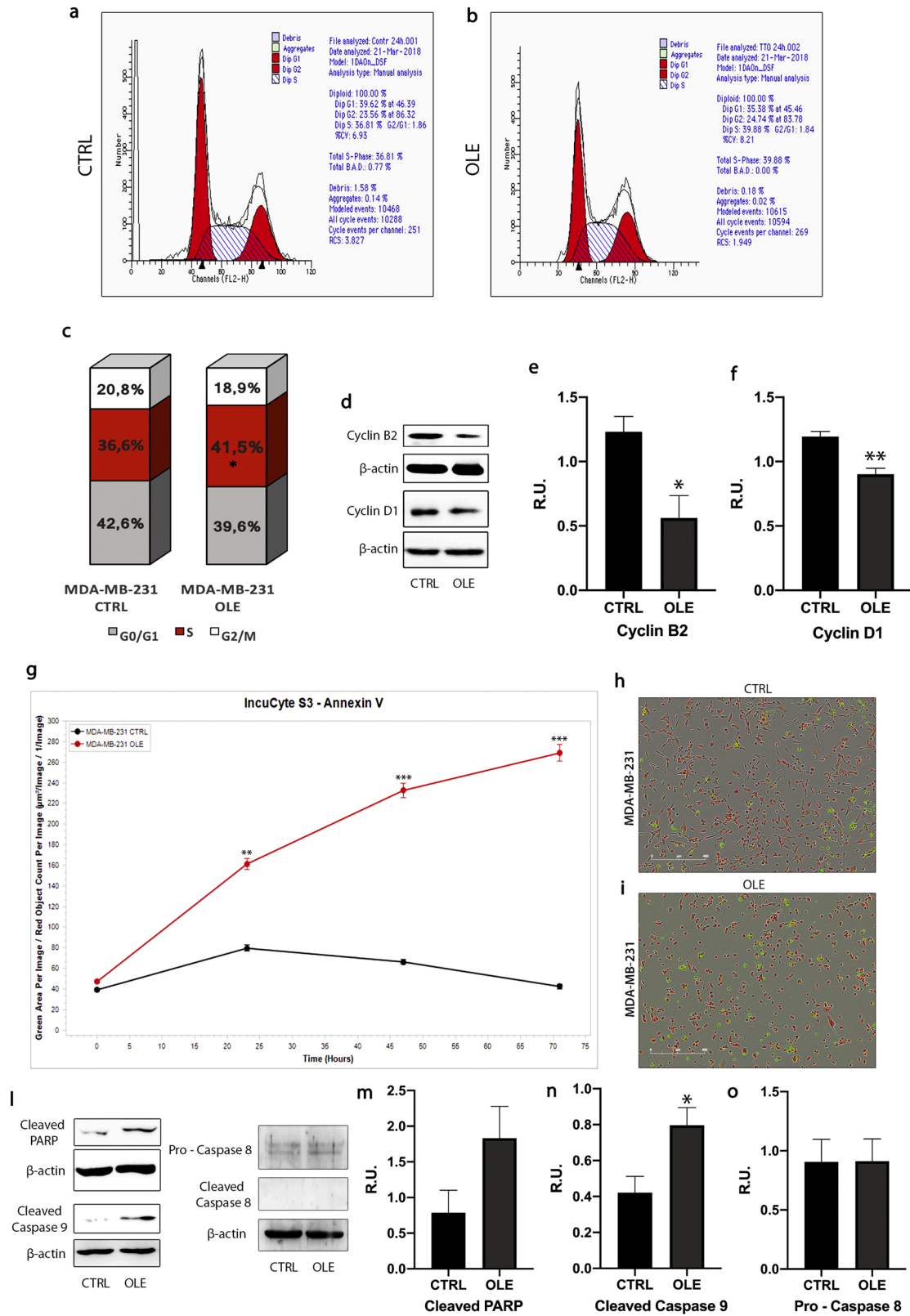
aggressive cancers among women. Nowadays, it is well-known the advantageous effect that the Mediterranean diet generates in human health at different levels. Recently, *Olea europaea* leaves have attracted increasing interest in the scientific society. Precisely, olive leaves constitute a discarded part of the plant, still remaining a non-edible product with a high nutritional and functional value that can be included as a co-adjuvant in antitumor therapy. On this basis, we studied OLE as a potential novel natural compound for the specific targeting of breast and ovarian cancer cells. So, in the interest of focusing on cancers of the female reproductive system, our findings confirm OLE ability to affect cell proliferation and apoptosis in breast cancer cells and provide, for the first time, strong experimental pieces of evidence on OLE selective ability to inhibit cell proliferation and to promote pro-apoptotic activity in ovarian cancer cells, through the production of intracellular and mitochondrial ROS and mitochondrial impairment, in agreement with recent findings indicating a pro-oxidant activity of polyphenols in cancer. Therefore, OLE might represent an attractive candidate for a positive lifestyle strategy for tumor prevention and drug development, sounding like a promising combined therapeutic strategy.

4. Results

4.1. OLE specifically inhibits the viability of MDA-MB-231 triple-negative breast and OVCAR-3 ovarian cancer cells

Firstly, a both qualitative and quantitative HPLC/DAD analysis on OLE have been performed to assess the total content of polyphenolics and other secondary metabolites. The main component of the extract was found to be oleuropein, and its quantity together with its derivatives, was assessed by means of the oleuropein calibration curve at 280 nm and it was found to be 87 % of the total components of the extract (Supplementary File 1). For assaying the antitumor effect of OLE, its influence on cell viability was evaluated in normal human corneal epithelial HCEpiC cells as well as in a panel of human breast (MDA-MB-231, MDA-MB-468) and ovarian cancer cell lines (OVCAR-3 and OVCAR-8). Cells were treated with increasing OLE concentrations from 100 to 400 $\mu\text{g/mL}$ for 24 h (Fig. 1) and 72 h (Supplementary Fig. 2), and IC_{50} values for all the tested cell lines were calculated. HCEpiC cells resulted only slightly affected, since around 90 % cell viability was still noticeable after 24 h at 400 $\mu\text{g/mL}$ OLE concentration (Fig. 1a), while

MDA-MB-231



(caption on next page)

Fig. 2. OLE induces cell cycle arrest and promotes apoptosis in MDA-MB-231 cells. MDA-MB-231 cells were exposed to OLE at 200 $\mu\text{g}/\text{mL}$ (b) or not (a) for 24 h, (a) and (b) are representative graphs of the experiment. The distribution of the cell cycle (c) was assessed by flow cytometry. For each sample, at least 2×10^5 events were analyzed (*, $p < 0.05$ versus control). (d) The levels of cell cycle regulatory proteins and relative densitometric analysis (e) (f) in MDA-MB-231 cells treated with OLE at 200 $\mu\text{g}/\text{mL}$ for 24 h were assessed by western blotting. β -actin was employed as a house-keeping for the equivalent loading of protein in the lanes; (g) InCuCyte quantification of MDA-MB-231 untreated cells (MDA-MB-231 CTRL, black line) and cells treated with OLE at 200 $\mu\text{g}/\text{mL}$ (MDA-MB-231 OLE, red line); (h) (i) Representative images of InCuCyte quantification in MDA-MB-231 untreated (h) and OLE treated (i) cells (in red, cells labeled with the InCuCyte® NucLight Rapid Red Reagent; in green, cells labeled with the InCuCyte® Annexin V Reagent); (j) MDA-MB-231 cells were incubated with OLE at 200 $\mu\text{g}/\text{mL}$ for 24 h. Cell lysates were obtained and then assayed by western blotting to evaluate the levels of apoptosis-related proteins. (m, n, o) The graphs show the relative densitometric analysis. The house-keeping protein β -actin has been employed as the loading control. For (c), (e), (f), (m), (n) and (o), statistical analysis was carried out by applying the unpaired Student's *t*-test. * $p < 0.05$; ** $p < 0.005$; *** $p < 0.0001$ vs CTRL. For (g), statistical analysis was carried out by applying the two-way analysis of variance (ANOVA) followed by Bonferroni's multiple comparisons test. Statistically significance was settled at ** $p < 0.005$, *** $p < 0.0001$ vs CTRL. Data are presented as mean \pm SEM of three different experiments; (n = 3). (For interpretation of the references to colour in the Figure, the reader is referred to the web version of this article).

MTS assay indicated an IC_{50} value very close to 200 $\mu\text{g}/\text{mL}$ after 24 h of treatment for MDA-MB-231 (Fig. 1b), MDA-MB-468 (Supplementary Fig. 2c), OVCAR-3 (Fig. 1c) and OVCAR-8 (Supplementary Fig. 2g), suggesting that OLE selectively targeted cancer cells. On this basis, the 200 $\mu\text{g}/\text{mL}$ concentration of OLE was chosen as the working concentration to be used for all the following experiments in both models. Additionally, OLE effectiveness was assessed by performing clonogenic assays to verify whether the compound was also able to exert a long-term cell growth inhibition. Data exhibited that OLE dramatically repressed the number of colonies formed in MDA-MB-231 (Fig. 1d,e), OVCAR-3 (Fig. 1f,g), MDA-MB-468 (Supplementary Fig. 2e,f) and OVCAR-8 cells (Supplementary Fig. 2i,l) after seven-ten days of treatment with three different concentration of OLE (100–50–25 $\mu\text{g}/\text{mL}$). These results confirmed the dose-response antiproliferative effect of the extract, verifying the ability of OLE to inhibit cell growth upon several breast and ovarian cancer models. In order to evaluate which component of the olive leaf extract could be responsible for the cytotoxic effect on cancer cell lines, the influence of the main bioactive component of the leaf extract, oleuropein, was assayed on MDA-MB-231 and OVCAR-3 cell viability. In agreement with recent findings demonstrating that oleuropein and hydroxytyrosol selectively reduce proliferation and induce apoptosis in pancreatic cancer cells [44], we confirmed that oleuropein was able to induce a cytotoxic effect on MDA-MB-231 and OVCAR-3 cells (Supplementary Fig. 3).

4.2. OLE promotes cell cycle arrest in MDA-MB-231 and OVCAR-3 cells

For studying OLE-mediated growth inhibition, since OLE did not affect HCEpiC cell viability, cell cycle through flow cytometric analysis was performed only in MDA-MB-231, OVCAR-3, MDA-MB-468 and OVCAR-8 cells exposed to 200 $\mu\text{g}/\text{mL}$ OLE for 24 h. As represented in Figs. 2 and 3, OLE induced a significant accumulation of cells in S phase in MDA-MB-231 (Fig. 2 a–c) and S-G2/M phase in OVCAR-3 (Fig. 3 a–c) cells. Specifically, the S phase population increased significantly from 36,9%–41,5% in MDA-MB-231 treated cells (Fig. 2c). Treatment of OVCAR-3 cells with 200 $\mu\text{g}/\text{mL}$ of OLE resulted in a significant increase in the percentage of S phase population from 21,3%–28,6% versus the untreated cells (Fig. 3c). The percentage of cells in the G2/M phase was also significantly higher in OVCAR-3 cells after treatment with 200 $\mu\text{g}/\text{mL}$ of OLE, from 12,2%–15% compared to the untreated cells (Fig. 3c). Preliminary data from experiments carried out in MDA-MB-468 and OVCAR-8 cells show a cell cycle arrest in S phases in MDA-MB-468 cells (Supplementary Fig. 4 a,c,d) and in OVCAR-8 cells (Supplementary Fig. 4b,e,f). Specifically, MDA-MB-468 cells, exposed to OLE, exhibited an accumulation of cells in the S phase from 14,9% to 29,5% compared with the control (Supplementary Fig. 4a), whereas OVCAR-8 cells showed an increment of cells in the S phase from 33,2% to 44,1% (Supplementary Fig. 4b). These preliminary data lead us to suppose an important block in S phases for MDA-MB-468 and OVCAR-8 cells. To further validate the results obtained by cytofluorimetry, by which OLE promotes cell cycle block at S and G2/M phases, the levels of two cell cycle essential regulatory proteins were analyzed by western blotting.

Fig. 2 d–f shows a significant decrease of cyclins D1 and B2 in OLE-treated MDA-MB-231 cells compared to untreated cells, while Fig. 3 d–f shows a significant reduction of cyclin B2. Still, no significant differences were detected for cyclin D1 in OVCAR-3 cells compared to control cells.

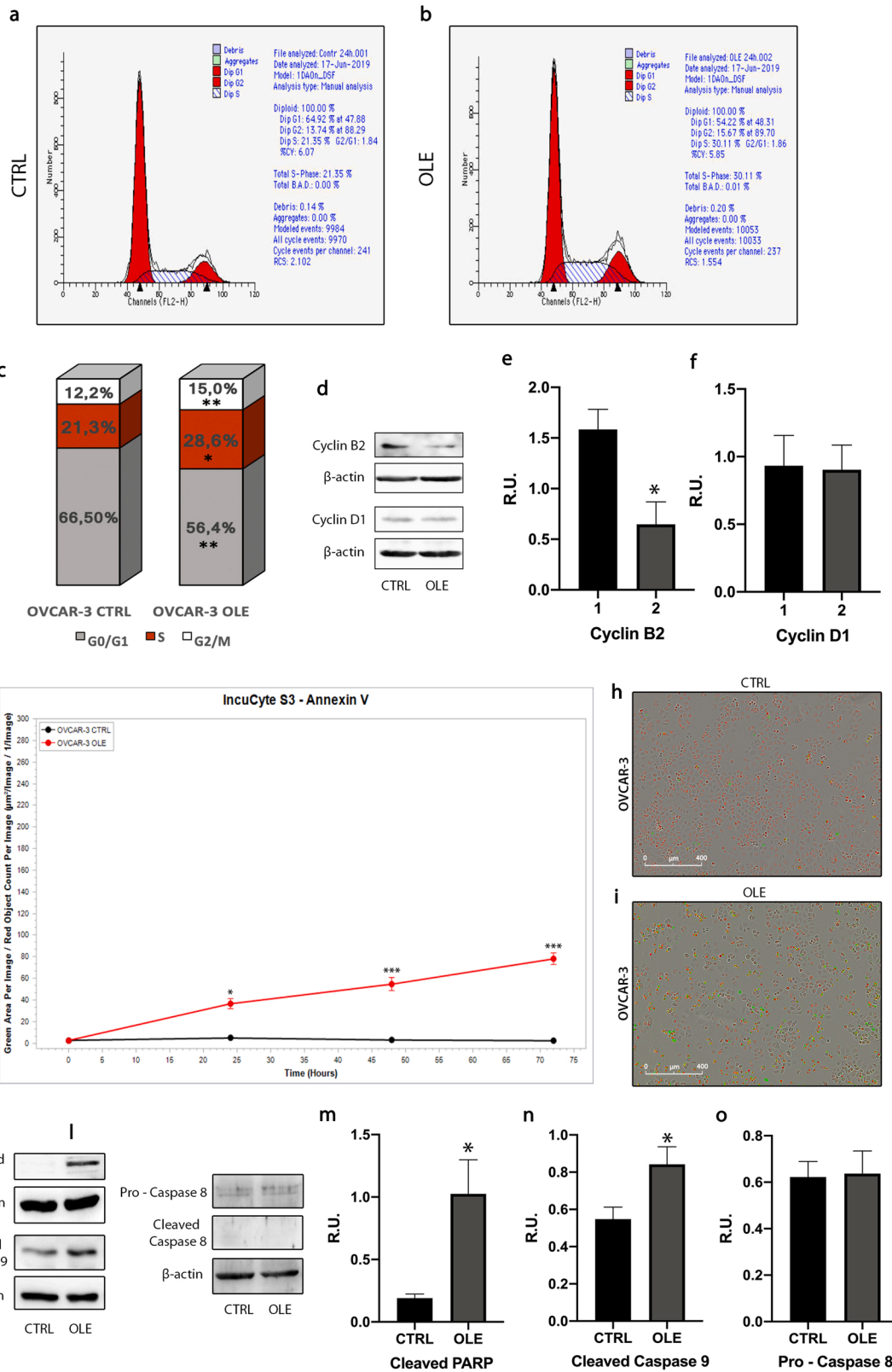
4.3. OLE promotes apoptosis in MDA-MB-231 and OVCAR-3 cells

To elucidate whether the cell cycle arrest upon OLE treatment was correlated to the induction of apoptosis, MDA-MB-231, and OVCAR-3 cells were treated with 200 $\mu\text{g}/\text{mL}$ OLE for 24 h, and the apoptotic progression was evaluated by performing an InCuCyte S3 live-cell Imaging System Analysis. OLE increased significantly apoptotic cells with respect to control cells, both in MDA-MB-231 and in OVCAR-3 cells, as shown in Fig. 2 g–i and Fig. 3 g–i. Also, our results also indicated apparent morphological changes associated with the apoptotic process in both models (Fig. 2 h,i; Fig. 3 h,i). For assaying the pathways involved in apoptosis-mediated cell death in our cancer models, the protein levels of cleaved caspase 9, cleaved PARP, pro-, and cleaved caspase 8 were investigated. Fig. 2 l–n and Fig. 3 l–n show that OLE promoted a notable increase in the expression of the initiator of the mitochondrial pathway caspase 9 and cleaved PARP, both in MDA-MB-231 (Fig. 2 l–n) and in OVCAR-3 (Fig. 3 l–n) cells. On the other hand, the protein levels of the initiator pro-caspase 8 remained unvaried. Additionally, it was not observed any activation of the p18 subunit, related to the cleaved form of the caspase 8, presuming that the membrane receptor-mediated extrinsic apoptotic pathway was not activated, because of the OLE treatment, within these cell tumor models (Fig. 2l,o and Fig. 3l,o). On the light of these results, our data pointed that OLE is able to strongly promote apoptosis in MDA-MB-231 and OVCAR-3 cells, probably exclusively throughout the activation of the intrinsic apoptotic pathway, as the initiator pro-caspase 8 did not show any type of regulation and any activation of its cleaved form upon the OLE treatment.

4.4. OLE affects apoptosis, selectively increasing ROS production and altering the protein levels of oxidative stress pathway-related proteins

It is well-known that high levels of ROS cause harmful oxidation in cells and control many cellular mechanisms, including apoptosis and cell cycle arrest, among others (47). Therefore, the DCFDA Cellular ROS Detection Assay Kit, monitoring intracellular ROS production by fluorescence detected by a microplate reader, was used in MDA-MB-231 and OVCAR-3 cells. The results showed that OLE treatment at 200 $\mu\text{g}/\text{mL}$ for 24 h significantly increased the intracellular ROS levels either in MDA-MB-231 (Fig. 4a) and in OVCAR-3 (Fig. 4b) cells. For counteracting ROS damaging effects, cells use antioxidant defense systems such as catalase and superoxide dismutase (SOD2). For this reason, the protein levels of these two crucial ROS scavengers were investigated. MDA-MB-231 (Fig. 4 c, e, f) and OVCAR-3 (Fig. 4 d, g, h) cells treated with OLE at 200 $\mu\text{g}/\text{mL}$ for 24 h show significant downregulation of protein expression level of SOD2 and catalase when compared to control cells. Furthermore, oxidative stress was significantly increased, as supported

OVCAR-3



(caption on next page)

Fig. 3. OLE induces cell cycle arrest and promotes apoptosis in OVCAR-3 cells. OVCAR-3 cells were exposed to OLE at 200 $\mu\text{g}/\text{mL}$ (**b**) or not (**a**) for 24 h; (**a**) and (**b**) are representative graphs of the experiment. The distribution of the cell cycle (**c**) was assessed by flow cytometry. For each sample, at least 2×10^5 events were analyzed (*, $p < 0.05$ versus control). (**d**) The levels of cell cycle regulatory proteins and relative densitometric analysis (**e**) (**f**) in OVCAR-3 cells treated with OLE at 200 $\mu\text{g}/\text{mL}$ for 24 h were assessed by western blotting. β -actin was employed as housekeeping for the equivalent loading of proteins in the lanes; (**g**) InCuCyte quantification of OVCAR-3 untreated cells (OVCAR-3 CTRL, black line) and cells treated with OLE at 200 $\mu\text{g}/\text{mL}$ (OVCAR-3 OLE, red line); (**h**, **i**) Representative images of InCuCyte quantification in OVCAR-3 untreated (**h**) and OLE treated (**i**) cells (in red, cells labeled with the InCuCyte® NucLight Rapid Red Reagent, that specifically stains nuclei in live cells and is ideally suited to the real-time quantification of cell counting; in green, cells labeled with the InCuCyte® Annexin V Reagent, thoroughly-specific phosphatidylserine (PS) cyanine fluorescent probe that is ideally designed for real-time apoptosis evaluation in living cultures); (**l**) OVCAR-3 cells were incubated with OLE at 200 $\mu\text{g}/\text{mL}$ for 24 h. Cell lysates were obtained and then assayed by western blotting to evaluate the levels of apoptosis-related proteins. (**m**, **n**, **o**) The graphs show the relative densitometric analysis. The house-keeping protein β -actin has been employed as the loading control. For (**c**), (**e**), (**f**), (**m**), (**n**) and (**o**), statistical analysis was carried out by applying the unpaired Student's *t*-test. * $p < 0.05$; ** $p < 0.005$; *** $p < 0.0001$ vs CTRL. For (**g**), statistical analysis was carried out by applying the two-way analysis of variance (ANOVA) followed by Bonferroni's multiple comparisons test. Statistically significance was settled at * $p < 0.05$, *** $p < 0.0001$ vs CTRL. Data are presented as mean \pm SEM of three different experiments; ($n = 3$). (For interpretation of the references to colour in the Figure, the reader is referred to the web version of this article).

by the levels of oxidized proteins determined by OxyBlot assay. As shown in Fig. 4i and 4L, in the OLE group, an increase in the expression of the oxidized protein was observed, both in MDA-MB-231 (Fig. 4i) and in OVCAR-3 (Fig. 4l) cells. These findings suggest that olive leaf extract acts as a pro-oxidant agent in MDA-MB-231 and OVCAR-3 cells. Given that OLE treatment in our conditions significantly inhibited cell viability, induced apoptosis, and increased intracellular ROS production in both MDA-MB-231 and OVCAR-3 cells, additional experiments were performed to examine whether OLE-induced cytotoxicity was mediated by the increase of intracellular ROS generation. To this purpose, cell viability and apoptosis were also investigated in the presence of NAC. NAC, an aminothiol that synthesizes the precursor of intracellular glutathione and cysteine, is considered an excellent antioxidant to prevent the generation of H_2O_2 [49]. HCEpiC, MDA-MB-231, and OVCAR-3 cells were treated or not with OLE at 200 $\mu\text{g}/\text{mL}$ for 24 h, with NAC alone at 5 nM, and in the presence of 1 h pre-treatment with 5 mM NAC and then OLE. By MTS assay, as shown in Fig. 5, we confirmed that OLE treatment significantly decreased cell viability both in MDA-MB-231 (Fig. 5b) and in OVCAR-3 (Fig. 5c) cells. In the presence of 5 mM NAC treatment, no significant changes occurred in terms of cell viability in any cancer model when compared to the control values. All pre-treatments with 5 mM NAC consistently impaired the OLE effects on cell viability both in MDA-MB-231 (Fig. 5b) and in OVCAR-3 (Fig. 5c) cells. In contrast, HCEpiC cells were not affected by OLE treatment, confirming again that OLE selectively targets cancer cells (Fig. 5a). Also, InCuCyte live-cell Imaging System analysis revealed that 5 mM NAC pretreatment completely counteracted the apoptotic effect of OLE, as detected by Annexin V staining both in MDA-MB-231 (Fig. 6c,d) and in OVCAR-3 (Fig. 6e,f) cells. Moreover, Fig. 6a,b shows that neither OLE nor NAC treatment has any effect on apoptosis in HCEpiC cells, confirming the safe ineffectiveness of our compound in non-tumoral cells. Overall, these evidences indicate that ROS production constitutes the mechanism underlying the ability of OLE to promote cell cycle arrest, apoptosis, and mitochondrial impairment in MDA-MB-231 and OVCAR-3 cells.

4.5. OLE compromises mitochondrial function

Previous investigations have shown that ROS production was strictly associated with mitochondrial impairment and membrane potential ($\Delta\Psi\text{m}$) changes [50,51]. Accordingly, the effect of OLE on the functional state of mitochondria and mitochondrial membrane potential changes were measured. Therefore, we performed a Fluorescence assay by using MitoTracker® Green FM probe after 24 h of OLE treatment. This fluorescent dye accumulates in active mitochondria by passively diffusing across the plasma membrane due to its low thiol-reactive chloromethyl moiety that allows mitochondria labeling. As observed in Fig. 7a and f, OLE caused a significant decrease of the fluorescence, thus suggesting an impairment of mitochondrial functionality or a reduction of mitochondrial number in MDA-MB-231 (Fig. 7a) and in OVCAR-3 (Fig. 7f) cells. The study was then extended to the evaluation of mitochondrial status

by using tetramethylrhodamine methyl ester (TMRM) to measure the mitochondrial membrane potential ($\Delta\Psi\text{m}$), a key indicator of mitochondrial health and the metabolic state of the cell. As shown in Fig. 7b and g, OLE treatment significantly resulted in $\Delta\Psi\text{m}$ loss in MDA-MB-231 (Fig. 7b) and OVCAR-3 (Fig. 7g) cells after 24 h of incubation. Our data were further validated by TMRM assay by using InCuCyte® live-cell imaging. Already at the first hours of treatment, OLE-treated MDA-MB-231 cells significantly showed a reduced basal $\Delta\Psi\text{m}$ compared to control cells (Fig. 7c-e), more accentuated in the OVCAR-3 model (Fig. 7h-l), suggesting the capacity of OLE in reducing the mitochondrial membrane potential, presumably leading to mitochondrial dysfunction and cell death, in agreement with the observed OLE-induced apoptosis. It is very well-known that oxidative stress is essentially produced in mitochondria [51], especially from mitochondrial superoxide. Therefore, we investigated the total amount of mitochondria-specific superoxide, measured using an oxygen radical-sensitive probe-MitoSOX upon OLE treatment, by using the InCuCyte live-cell Imaging System. MitoSOX analyses showed a significant increase in mitochondrial superoxide generation after OLE treatment at 200 $\mu\text{g}/\text{mL}$ for 24 h, both in MDA-MB-231 (Fig. 8c,d) and in OVCAR-3 (Fig. 8e,f) cells. Furthermore, OLE-induced MitoSOX generation in MDA-MB-231 and OVCAR-3 cells was suppressed by the treatment with 5 mM NAC; in fact, pre-treatment with NAC significantly inhibited mitochondrial superoxide generation both in MDA-MB-231 (Fig. 8c,d) and in OVCAR-3 (Fig. 8e,f) cells. Fig. 8a,b shows that OLE and NAC treatment, neither alone nor together, did not produce significant changes in the mitochondrial superoxide production in HCEpiC cells, suggesting that OLE pro-oxidant effects are specific for cancer cells.

5. Discussion

Breast cancer is the most common cancer among women, registering 2,1 million women each year, and is also responsible for the greatest number of cancer-related deaths among women all over the world [1]. Ovarian cancer, instead, represents the most lethal gynecological cancer in the world. Ovarian tumor is significantly less frequent than breast cancer but considerably more aggressive. The huge mortality rate is mostly associated with its unknown progression, resulting in fast-developed, diffused malignancy involving about 75 % of women at diagnosis [52]. Many studies have concentrated on the antiproliferative effect of single drugs or natural compounds by performing detailed analysis of cell proliferation signaling or metabolic pathways [53]. It is well-known, nowadays, the beneficial effects that the Mediterranean diet generates in human health at different levels. In this regard, immunomodulatory, anti-diabetic, anti-cardiovascular, anti-inflammatory, or anti-infective and anti-microbial actions have been associated with correcting dietary habits in individuals who adhere to the Mediterranean Alimentary culture. Recently, *Olea europaea* leaves have attracted increasing interest in the scientific society. Therefore, the industry put considerable effort into exploiting this agricultural waste [22]. Precisely, olive leaves constitute a discarded part of the plant that

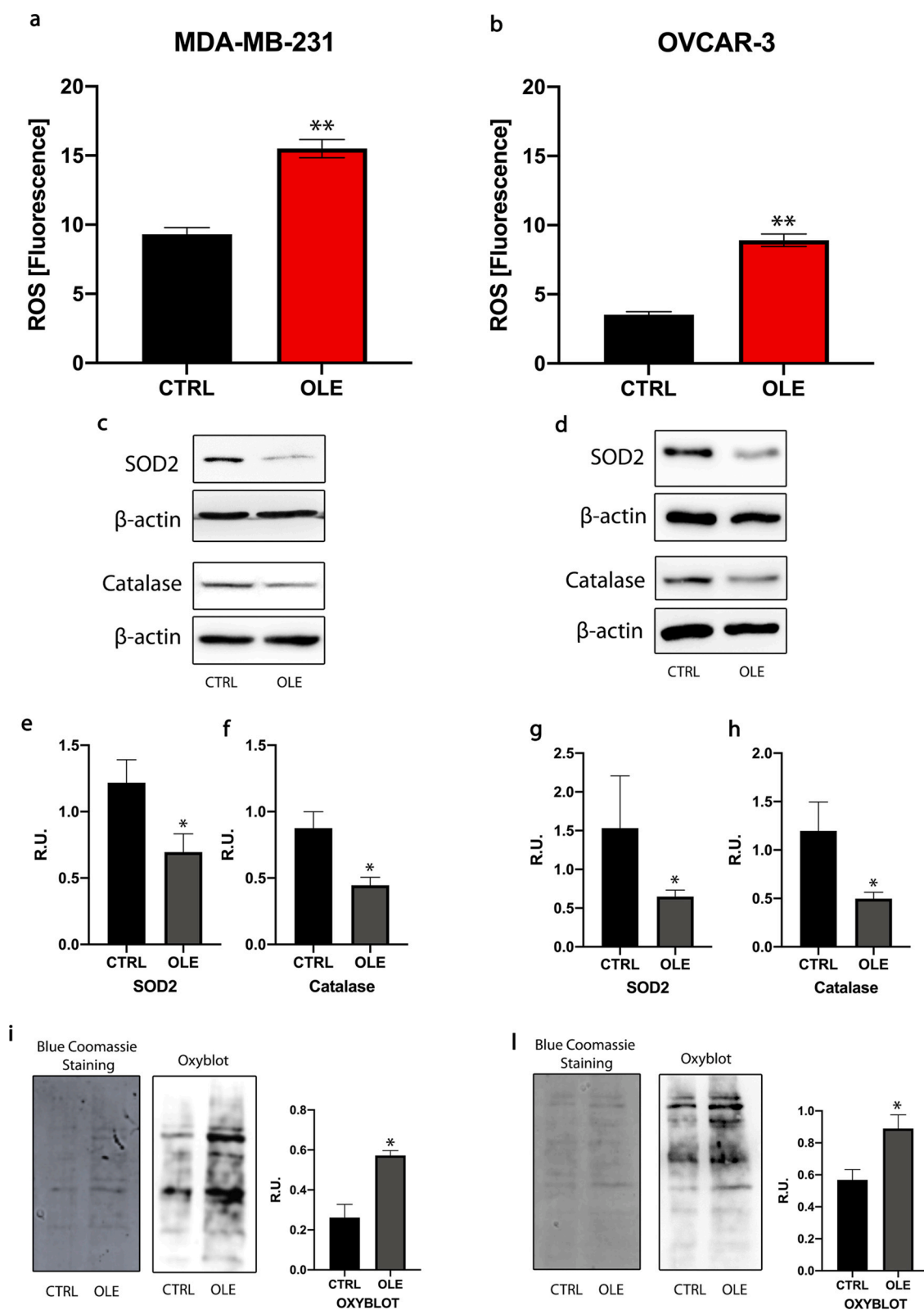


Fig. 4. OLE increases ROS accumulation and affects the protein levels of oxidative stress pathway-related proteins in MDA-MB-231 and OVCAR-3 cells. MDA-MB-231 (a) and OVCAR-3 (b) cells were incubated for 24 h with or without OLE at 200 μ g/mL, and ROS were detected with DCFDA Cellular ROS detection Assay Kit, and fluorescence intensity was calculated using a Victor3 microplate reader. (c-h) Western blotting and relative densitometric analysis for the protein levels of oxidative stress pathway-related proteins in MDA-MB-231 (c, e, f) and OVCAR-3 (d, g, h) cells; (i, l) Evidence of increased oxidative stress and relative densitometric analysis in MDA-MB-231 (i) and OVCAR-3 (l) cells treated with OLE at 200 μ g/mL for 24 h. OxyBlot Protein Oxidation Detection Kit was employed for detecting the carbonyl groups introduced by oxidative reactions into the proteins in MDA-MB-231 (i) and OVCAR-3 (l) cells by immunoblotting. Statistical analysis was carried out by employing the unpaired Student's *t*-test. * $p < 0.05$; ** $p < 0.005$; *** $p < 0.0001$ vs CTRL. Data are presented as mean \pm SEM of three different experiments; (n = 3).

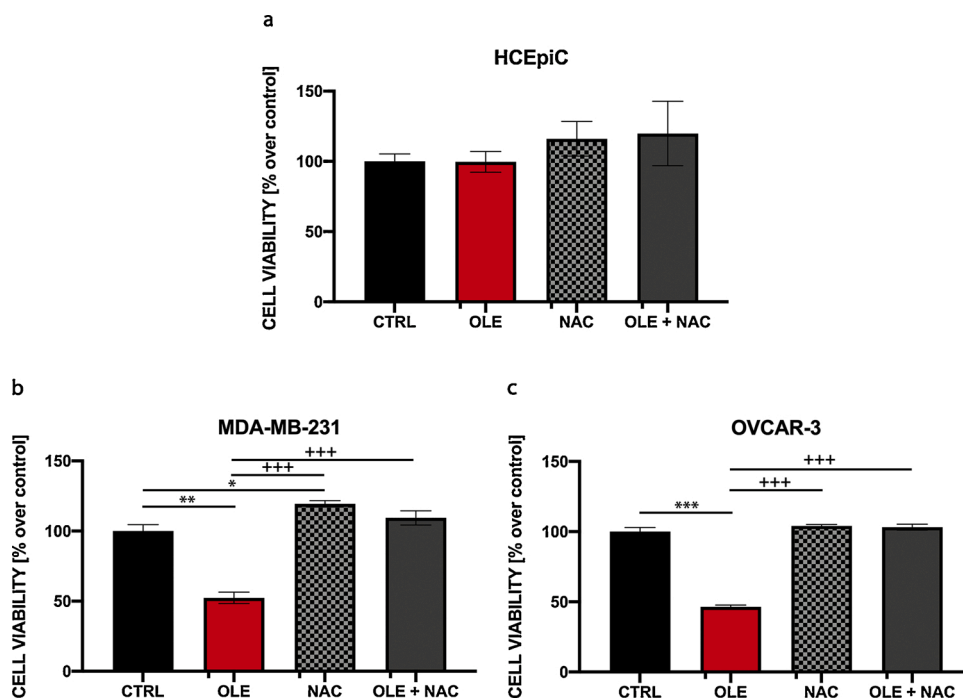


Fig. 5. OLE affects cell viability through the activation of ROS in MDA-MB-231 and in OVCAR-3 cells. To examine whether OLE-induced cytotoxicity was mediated by the increase of intracellular ROS generation, the effect of NAC on cell viability has been investigated. HCEpiC, MDA-MB-231, and OVCAR-3 cells were treated or not with OLE at 200 $\mu\text{g}/\text{mL}$ for 24 h, with 5 mM NAC, or pretreated with 5 mM NAC 1 h before the treatment with OLE at 200 $\mu\text{g}/\text{mL}$ for additional 24 h. The MTS assay was performed in HCEpiC (a), MDA-MB-231 (b), and in OVCAR-3 (c) cells. Statistical analysis was carried out by applying the one-way analysis of variance (ANOVA) followed by Tukey post hoc tests for multiple comparisons. Statistical significance was settled at * $p < 0.05$, ** $p < 0.005$, vs CTRL; +++ $p < 0.0001$ vs OLE. Data are presented as mean \pm SEM of three different experiments; ($n = 3$).

nowadays remains a non-edible product with a high nutritional and functional value that can be included as a co-adjuvant in antitumor therapy. Moreover, many pieces of research have underlined the anticancer potential of olive leaf extracts, focusing on the inhibition of cell proliferation in MDA-MB-231 [19–21], MCF-7 [20–23], SKBR3 [22], and JIMT-1 [24] breast cancer cell lines. Nevertheless, scientists are now focusing their studies on the molecular mechanisms and the specific compound -or mixture of them- responsible for their anti-tumoral properties. Recently, the request for olive leaf extract has expanded because of its use in foodstuffs, food additives, and functional food materials [54]. Polyphenols are present in OLE as a mixture, and much evidences indicate that OLE polyphenols act synergistically, resulting in an increased effect with respect to the effect of the single polyphenol [33,55,56]. For this reason, it appears more appropriated to use the extract rather than the single components to evaluate the bioactive effects. Moreover, it appears that OLE polyphenols can discriminate between normal and the cancer cell, rendering more interesting their use as co-adjuvant compounds [19,57]. Our study confirmed OLE anti-proliferative and pro-apoptotic role on human TNBC and, for the first time, demonstrated that OLE exerted a pro-apoptotic activity on human ovarian tumor cells, providing exploratory data on the involved mechanisms. Our results show that OLE causes effectively and selectively a dose-dependent reduction of cell viability in MDA-MB-231 and OVCAR-3 cells, exerting a pro-oxidant cytotoxic effect on these cell lines. These results are in agreement with several recent studies demonstrating that natural compounds including alpinumisoflavone, laburnetin, amentoflavone [58] or abyssinone IV, atalantoflavone [59], isoliensinine [60], physagulide [61], Ziyuglycoside [62], Crocin [63] and annurca apple polyphenol extract [64] are capable of enhancing ROS production in MDA-MB-231 cells specifically. This pro-oxidant effect assigned to plant-derived phytochemicals is becoming an innovative finding closely linked to the antitumor mechanisms exerted by these compounds, which has additionally be hypothesized to be one of the key points unleashing the apoptotic process and cell cycle block in cancer cells [63]. By performing a HPLC/DAD analysis on our extract, the main component of the extract was found to be oleuropein, with a percentage of 87 % of the total extract. The used OLE concentration is in agreement with the literature studies on MDA-MB-231 cells and also with other studies on different cancer models, such as pancreatic or leukemia [19,

21,26,29,44,65,66]. Moreover, it has been previously emphasized that, even analyzing the same cancer model, the effect of OLE is lineage-specific [19,65,66]. Also, there are many other pieces of evidence about the capacity of natural compounds such as costunolide [67] and gallic acid [68] to cause an increment of ROS levels in ovarian cancer cells too. On this basis, we studied OLE as a potential novel natural compound for the specific targeting of breast and ovarian cancer cells. By evaluating the potential role of OLE as a powerful cell death inducer, we investigated the effect of the extract on cell cycle progression. Our data revealed that OLE induced a significant accumulation of cells in S phase in MDA-MB-231 and S and G2/M phases in OVCAR-3 cells. These results were further confirmed by a significant decrease of cyclins B2 and D1 in MDA-MB-231 cells compared to untreated cells, and a significant decrease only of cyclin B2 in OVCAR-3 cells compared to control cells, verifying a significant inhibitory impact on the expression levels of proteins associated with cell cycle progression and cell survival. Indeed, Cyclin D1 proto-oncogene is an important regulator of the G1 to S cell cycle phase checkpoint that has been shown to be involved in the development of endocrine resistance in breast cancer cells [69], which downregulation has already been demonstrated in colon and breast tumors following several drug's administration, including plant-derived polyphenols [70]. On the other hand, Cyclin B is a master regulator of the cell entrance to mitosis, leading the G2 to M cell cycle progression and so being strongly involved in cell division and proliferation. It is worth noting that in breast cancer, elevated levels of cyclin B2 represent a negative prognostic factor [71]. Moreover, by using different datasets available, through an OncoPrint analysis of core serous epithelial ovarian cancer genes, it has been demonstrated that cyclin B2 was upregulated in cancer versus normal tissue, suggesting its role as a potential therapeutic target [72]. In our cancer models, data revealed that OLE could trigger the mitochondrial-mediated intrinsic apoptotic pathway, as confirmed by the up-regulation of protein levels of the examined apoptosis-related markers cleaved caspase 9 and cleaved PARP, and by IncuCyte cell-live imaging system. The absence of the modulation of the full-length pro-caspase 8 protein levels and the lack of the activation of the cleaved form of caspase 8 lead us to suppose that the olive leaf extract did not exert its main antitumor function throughout the extrinsic apoptotic pathway. Moreover, we obtained direct demonstrations that ROS production was the first mechanism of

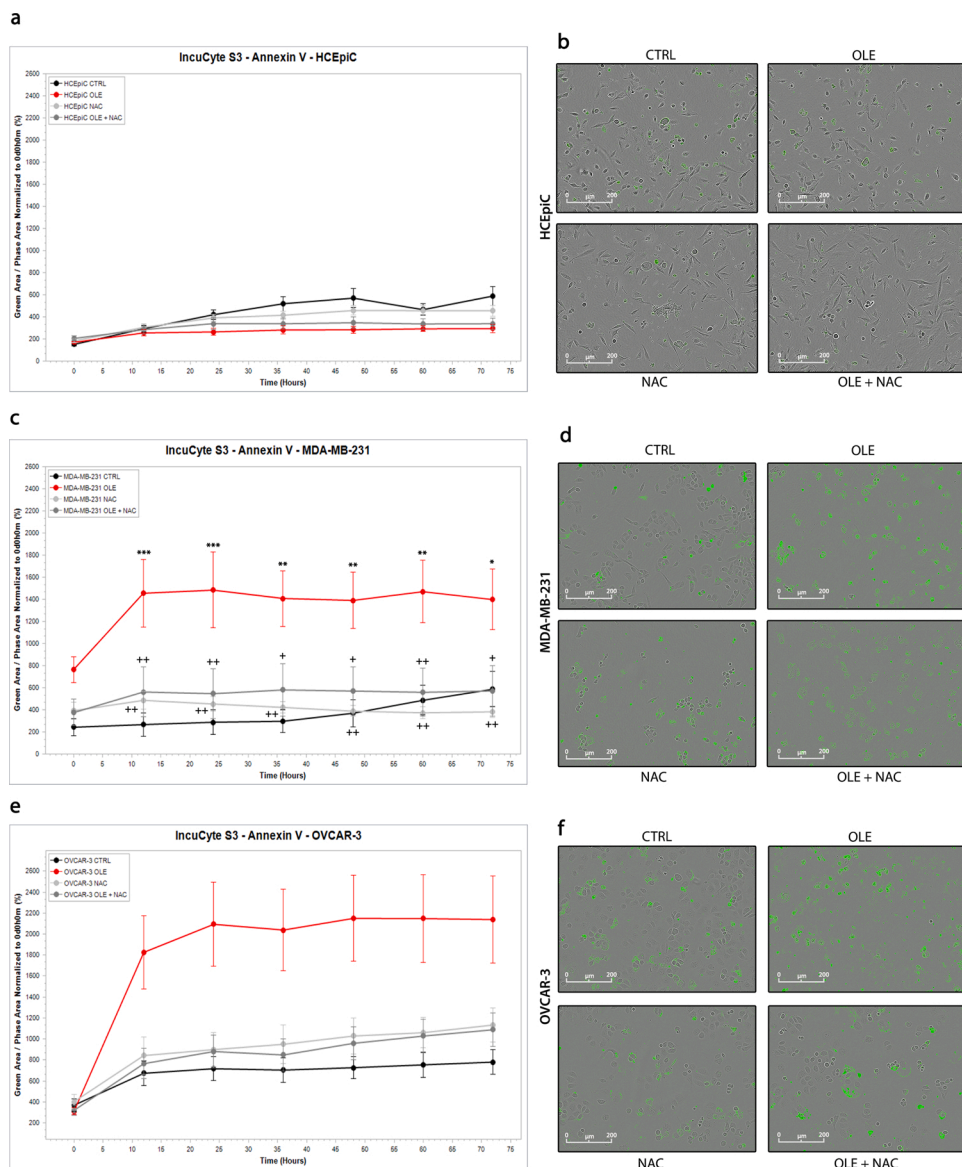


Fig. 6. OLE promotes apoptosis in MDA-MB-231 and OVCAR-3 cells. (a-f) HCEpiC, MDA-MB-231, and OVCAR-3 cells were treated or not with OLE at 200 µg/mL for 24 h, with 5 mM NAC, and pre-treated with 5 mM NAC 1 h before the treatment with OLE at 200 µg/mL for additional 24 h. IncuCyte quantification of HCEpiC (a, b), MDA-MB-231 (c, d) and OVCAR-3 (e, f) cells labeled with the IncuCyte® Annexin V Reagent; (b, d, f) Representative images of IncuCyte quantification in of HCEpiC (b), MDA-MB-231 (d) and OVCAR-3 (f) cells labeled with the IncuCyte® Annexin V Reagent. Statistical analysis was carried out by applying the two-way analysis of variance (ANOVA) followed by Tukey post hoc tests for multiple comparisons. Statistical significance was settled at * p < 0.05, ** p < 0.005, *** p < 0.0001 vs CTRL; + p < 0.05, ++ p < 0.005, +++ p < 0.0001 vs OLE. Data are presented as mean ± SEM of three different experiments; (n = 3).

OLE antitumoral effects in MDA-MB-231 and OVCAR-3 cells. Pretreatment with NAC, a ROS scavenger, abolished the inhibition of cell proliferation, cell cycle arrest, and apoptosis induced by OLE treatment. We found that NAC was able to revert the apoptotic effect of OLE, suggesting that apoptotic pathways are regulated by ROS production. The different number of apoptotic cells observed between all cell lines arises as a consequence of the different cell size, seeding density, and proliferation ratio, influencing the maximum number of cells and the related apoptotic events per field. Emerging findings demonstrate that polyphenols also have pro-oxidant activities, and they may regulate several signaling pathways responsible for antiproliferative and pro-apoptotic activity on pre-neoplastic and neoplastic cells [39]. ROS have a crucial role in carcinogenesis and are responsible for the action of many chemotherapeutic drugs. On the other hand, pro-oxidant compounds could exert their cytotoxic effect by enhancing the levels of ROS in tumoral cells beyond critical threshold limitation [42]. Cancer cells, in a condition of increased oxidative stress, are more responsive to ROS respect to normal cells. Accordingly, the increase of ROS induced by polyphenols action may be an efficient approach to kill cancer cells [43]. When ROS are present at a very high concentration, they can cause damage to DNA, lipids, or proteins, contributing to cytotoxicity in cells [73]. Our study shows that ROS production induced by OLE was

awe-inspiring, overcoming the antioxidant ability of ROS scavenging enzymes, SOD2, and catalase, which resulted significantly down-regulated in MDA-MB-231 and OVCAR-3 cells. These findings were supported by OxyBlot analysis showing that OLE treatment displays pro-oxidative effects in both cancer models.

Mitochondria play a pivotal role in cancer metabolic reprogramming [74,75]. Other than regulating energetics metabolism, mitochondria represent the central point of control of epigenetics, stemness, and initiation of apoptosis [76,77]. This aspect allows them to represent a sensor for endogenous stress contributing to cell adaptation to challenging microenvironments, giving elevated plasticity to tumor cells for growth and survival. In any case, there is not a single role for mitochondria in tumorigenesis and cancer progression and response to anti-cancer treatments. Indeed, mitochondrial functions may behave differently in various cancer on the basis of differences in genetics, microenvironments, and tumor type. Sometimes also in the same tumor, different populations of tumor cells may play different mitochondrial functions enabling tumor adaptation and therapeutic failure. In light of the central role that mitochondria play in cancer progression, presently, it has been proposed the term “mitochondrial medicine” [78]. Mitochondrial dysfunction in cancer cells may represent a good choice for specific anti-cancer therapy. In recent years, the term “mitocans” has

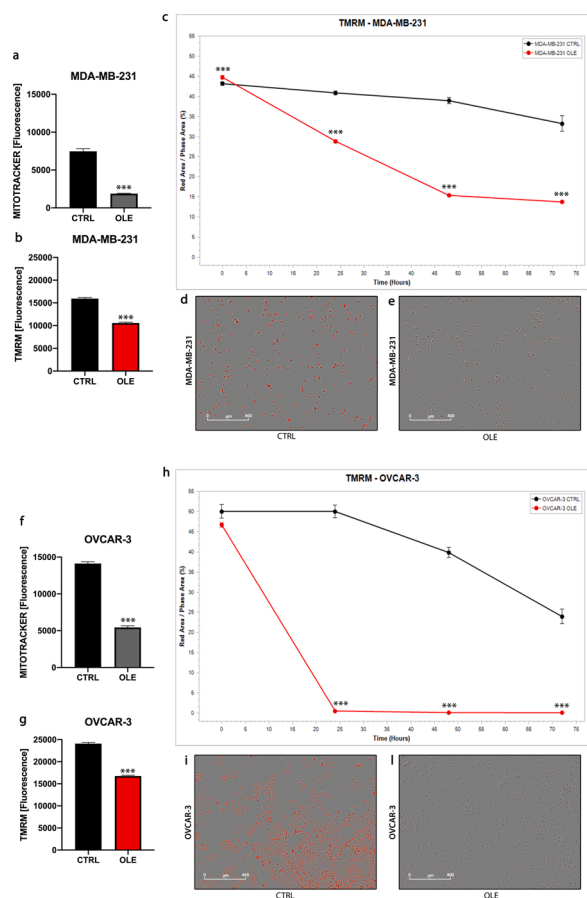


Fig. 7. OLE compromises mitochondrial mass and causes mitochondrial membrane potential ($\Delta\Psi_m$) loss in MDA-MB-231 and OVCAR-3 cells. (a, f) Measurement of mitochondrial mass by using MitoTracker® Green FM probe. MDA-MB-231 and OVCAR-3 cells, after treatment with OLE at 200 $\mu\text{g}/\text{mL}$ for 24 h, were incubated for 30 min at 37 °C with 200 nM MitoTracker® Green FM probe. Fluorescence was immediately measured in MDA-MB-231 (a) and in OVCAR-3 (f) cells by using a Victor3 microplate reader; (b, g) Changes in mitochondrial membrane potential ($\Delta\Psi_m$) were recorded with TMRM. MDA-MB-231 (b) and OVCAR-3 (g) cells were loaded with 100 nM TMRM for 30 min at RT. Fluorescence was immediately measured using a Victor3 microplate reader; (c-e) (h-l) Additional fluorescent analysis with TMRM was carried out by using IncuCyte® S3 Live-Cell Analysis System. After washing with complete fresh media, fluorescence was measured in MDA-MB-231 (c) and OVCAR-3 (h) cells on the IncuCyte® S3 Live-Cell Analysis System. Cell images were taken by using phase contrast and red channel (400 ms exposure) in the IncuCyte ZOOM™ platform. (d, e) Representative images of MDA-MB-231 untreated (d) and treated with OLE at 200 $\mu\text{g}/\text{mL}$ (e) for 24 h, stained with TMRM by using live cell analysis. Graphics were created with basic software graph functions (Essen Bioscience); (i, l) Representative images of OVCAR-3 untreated (i) and treated with OLE at 200 $\mu\text{g}/\text{mL}$ (l) for 24 h stained with TMRM by using live cell analysis. Graphics were created with basic software graph functions (Essen Bioscience). For (a), (b), (f), and (g), statistical analysis was carried out by applying the unpaired Student's *t*-test. * $p < 0.05$; ** $p < 0.005$; *** $p < 0.0001$ vs CTRL. For (c) and (h), statistical analysis was carried out by applying the two-way analysis of variance (ANOVA) followed by Bonferroni's multiple comparisons test. Statistical significance was settled at *** $p < 0.0001$ vs CTRL. Data are presented as mean \pm SEM of three different experiments; (n = 3). (For interpretation of the references to colour in the Figure, the reader is referred to the web version of this article).

been proposed for mitochondrial drugs targeting cancer cells, classified on their action [79]. These drugs may target directly mitochondria or metabolic pathways or trigger a retrograde signal, as increased ROS levels, targeting specific molecular alterations resulting from activation of the retrograde mitochondrial signaling may provide a selective

therapeutic approach for cancers. The novel finding of this study never reported previously to our knowledge is that OLE treatment inefficiency the functional state of mitochondria and mitochondrial membrane potential and significantly increased mitochondrial ROS levels selectively in MDA-MB-231 and OVCAR-3 cells. While in MDA-MB-231 and OVCAR-3 cells, OLE led to a significant increment of mitochondrial ROS levels with respect to untreated control cells, no mitochondrial ROS increase was observed in HCEpiC cells, indicating that the generation of ROS was specific for cancer cells. Furthermore, the obtained data confirmed that MDA-MB-231 and OVCAR-3 cells displayed an evident basal level of ROS compared with that of HCEpiC cells, reinforcing the hypothesis that tumor cells have typically greater levels of ROS versus healthy cells. The other new aspect is that OLE-induced cytotoxicity appears to involve mitochondrial ROS signaling. With this aim, to elucidate the underlying cytotoxic mechanisms induced by OLE, we observed that pretreatment with the antioxidant NAC significantly decreased OLE-induced mitochondrial superoxide production and cytotoxicity. Specifically, all NAC pretreatments reduced OLE impact on cell viability and mitochondrial superoxide production, similarly in both tumoral cell lines analyzed, without injuring healthy cells, confirming again the OLE targeted activity on cancer cells. In conclusion, our study highlights olive leaf extract -OLE- as a functional compound able to regulate cell growth of triple-negative breast MDA-MB-231 and ovarian OVCAR-3 cancer cells. It proposes a mechanistic explanation involving ROS production (mainly mitochondrial superoxide) and mitochondrial impairment. The novelty of this study relies on two important aspects: 1) the effects of OLE on ovarian cancer cells has never been previously studied, and we now add significant results on the effects of OLE on this cancer; 2) the induction by OLE of mitochondrial dysfunction was never assessed previously, supporting our finding on the OLE ability to affect cell proliferation and apoptosis in MDA-MB-231 cells and providing, for the first time, solid experimental pieces of evidence on the mechanisms promoting OLE selective ability to inhibit cell proliferation and to promote pro-apoptotic activity in OVCAR-3 cells. Therefore, the pleiotropic roles of OLE on tumor cells deserve attention and might represent an attractive candidate for a positive food habit strategy for tumor prevention and drug development for breast and ovarian cancer. However, OLE effects on cancer should be strengthened by further preclinical and clinical studies. Future investigations will involve experimental animal models to validate these data and to understand the adjuvant efficacy of OLE in combination with gold standard therapies.

Funding

This research was funded by Horizon 2020 MSCA-COFUND Rep-Eat Program; Grant Agreement n 713714. This work was supported by the A. I.M. Project-PON R & I 2014-2020 No. AIM11CC745-2, CUP E18H1900033007.

CRedit authorship contribution statement

Reyes Benot-Dominguez: Conceptualization, Methodology, Validation, Investigation, Writing - original draft, Visualization. **Maria Grazia Tupone:** Conceptualization, Methodology, Validation, Investigation, Writing - original draft. **Vanessa Castelli:** Methodology, Validation, Visualization. **Michele d'Angelo:** Software, Formal analysis, Data curation. **Elisabetta Benedetti:** Investigation, Writing - original draft. **Massimiliano Quintiliani:** Visualization. **Benedetta Cinque:** Methodology. **Iris Maria Forte:** Methodology, Visualization. **Maria Grazia Cifone:** Writing - review & editing, Supervision. **Rodolfo Ippoliti:** Writing - review & editing, Supervision. **Barbara Barboni:** Writing - review & editing, Supervision, Project administration, Funding acquisition. **Antonio Giordano:** Writing - review & editing, Supervision. **Annamaria Cimini:** Resources, Writing - review & editing, Supervision, Funding acquisition.

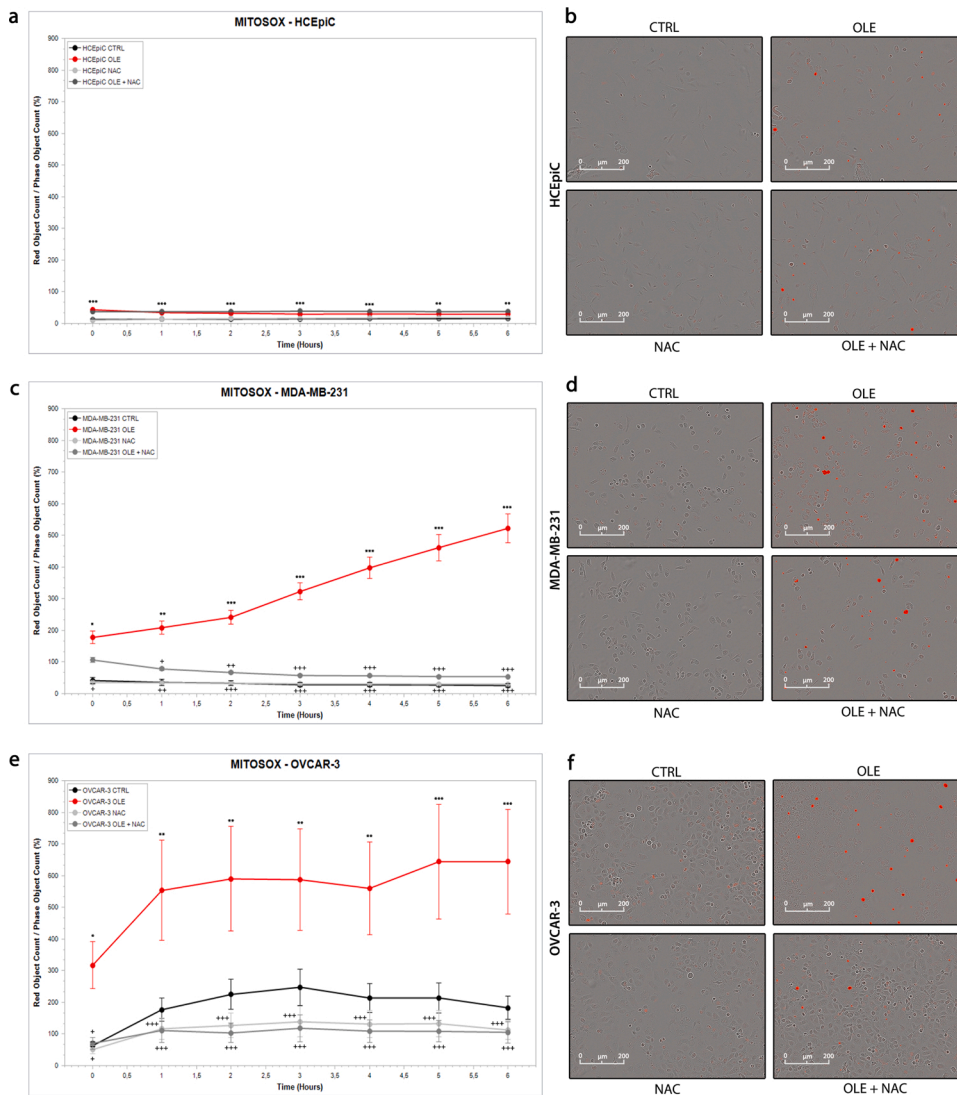


Fig. 8. OLE increases the level of mitochondrial superoxide in MDA-MB-231 and in OVCAR-3 cells. (a-f) HCEpiC, MDA-MB-231, and OVCAR-3 cells were treated or not with OLE at 200 $\mu\text{g}/\text{mL}$ for 24 h, with 5 mM NAC, and pre-treated with 5 mM NAC 1 h before the treatment with OLE at 200 $\mu\text{g}/\text{mL}$ for additional 24 h. After 24 h of OLE treatment, the level of mitochondria-specific reactive oxygen species (ROS) was monitored up to 6 h and quantified with the oxygen radical-sensitive probe-MitoSOX, by using the IncuCyte live-cell Imaging System. MitoSOX analyses were performed in HCEpiC (a, b), MDA-MB-231 (c, d), and OVCAR-3 (e, f) cells after the OLE treatment at 200 $\mu\text{g}/\text{mL}$ for 24 h. (b, d, f) Representative images of IncuCyte quantification in HCEpiC (b), MDA-MB-231 (d), and OVCAR-3 (f) cells labeled with the oxygen radical-sensitive probe-MitoSOX. Statistical analysis was carried out by applying the two-way analysis of variance (ANOVA) followed by Tukey post hoc tests for multiple comparisons. Statistical significance was settled at * $p < 0.05$, ** $p < 0.005$, *** $p < 0.0001$ vs CTRL; + $p < 0.05$, ++ $p < 0.005$, +++ $p < 0.0001$ vs OLE. Data are presented as mean \pm SEM of three different experiments; (n = 3). For more details, the complete statistical analysis related to Fig. 8a is presented in Supplementary Material Fig. 5.

Declaration of Competing Interest

The authors report no declarations of interest.

Acknowledgments

This study was possible thanks to the support of the Horizon 2020 MSCA-COFUND Rep-Eat Program and the A.I.M. Project-PON R & I 2014-2020. The authors would like to also thank the Center for Microscopy at the University of L'Aquila, headed by Prof. Luca Lozzi and the company Oleafit S.R.L. (Isola del Gran Sasso D'Italia, TE, Italy) for providing us the Olive leaf extract to carry out our experiments.

Appendix A. Supplementary data

Supplementary material related to this article can be found, in the online version, at doi:<https://doi.org/10.1016/j.biopha.2020.111139>.

References

- N. Li, Y. Deng, L. Zhou, T. Tian, S. Yang, Y. Wu, Y. Zheng, Z. Zhai, Q. Hao, D. Song, D. Zhang, H. Kang, Z. Dai, Global burden of breast cancer and attributable risk factors in 195 countries and territories, from 1990 to 2017: results from the Global Burden of Disease Study 2017, *J. Hematol. Oncol.* 12 (2019) 140, <https://doi.org/10.1186/s13045-019-0828-0>.
- L.A. Torre, B. Trabert, C.E. DeSantis, K.D. Miller, G. Samimi, C.D. Runowicz, M. M. Gaudet, A. Jemal, R.L. Siegel, Ovarian cancer statistics, 2018: ovarian cancer statistics, 2018, *CA Cancer J. Clin.* 68 (2018) 284-296, <https://doi.org/10.3322/caac.21456>.
- Y. Barak, D. Fridman, Impact of mediterranean diet on cancer: focused literature review, *Cancer Genomics Proteomics* 14 (2017) 403-408, <https://doi.org/10.21873/cgp.20050>.
- A. Trichopoulou, P. Lagiou, H. Kuper, D. Trichopoulos, *Cancer and Mediterranean dietary traditions, cancer epidemiol, Biomarkers Prev.* 9 (2000) 869-873.
- P. De Cicco, M.V. Catani, V. Gasperi, M. Sibilano, M. Quaglietta, I. Savini, Nutrition and breast cancer: a literature review on prevention, treatment and recurrence, *Nutrients* 11 (2019) 1514, <https://doi.org/10.3390/nu11071514>.
- A. Seiler, M.A. Chen, R.L. Brown, C.P. Fagundes, Obesity, dietary factors, nutrition, and breast cancer risk, *Curr. Breast Cancer Rep.* 10 (2018) 14-27, <https://doi.org/10.1007/s12609-018-0264-0>.
- C.M. Olsen, A.C. Green, D.C. Whiteman, S. Sadeghi, F. Kolahdooz, P.M. Webb, Obesity and the risk of epithelial ovarian cancer: a systematic review and meta-analysis, *Eur. J. Cancer* 43 (2007) 690-709, <https://doi.org/10.1016/j.ejca.2006.11.010>.
- A. Smits, A. Lopes, N. Das, R. Bekkers, K. Galaal, Quality of life in ovarian cancer survivors: the influence of obesity, *Int. J. Gynecol. Cancer* 25 (2015) 616-621, <https://doi.org/10.1097/IGC.0000000000000388>.
- K.W. Foong, H. Bolton, Obesity and ovarian cancer risk: a systematic review, *Post Reprod. Health* 23 (2017) 183-198, <https://doi.org/10.1177/2053369117709225>.
- A.T. Fleischauer, N. Simonsen, L. Arab, Antioxidant supplements and risk of breast cancer recurrence and breast cancer-related mortality among postmenopausal women, *Nutr. Cancer* 46 (2003) 15-22, https://doi.org/10.1207/S15327914NC4601_02.
- A. Sannella, F. Ieri, A. Romani, F. Vincieri, L. Messori, G. Maiori, C. Severini, A. Bilia, Modulation of the in vitro antimalarial effects of artemisinin by selected extracts: the case of olive leaf water extract, *Planta Med.* 74 (2008) s-0028-1084205, <https://doi.org/10.1055/s-0028-1084205>.

- [12] H.K. Hamdi, R. Castellon, Oleuropein, a non-toxic olive iridoid, is an anti-tumor agent and cytoskeleton disruptor, *Biochem. Biophys. Res. Commun.* 334 (2005) 769–778, <https://doi.org/10.1016/j.bbrc.2005.06.161>.
- [13] K. Qabaha, F. AL-Rimawi, A. Qasem, S.A. Naser, Oleuropein is responsible for the major anti-inflammatory effects of olive leaf extract, *J. Med. Food* 21 (2018) 302–305, <https://doi.org/10.1089/jmf.2017.0070>.
- [14] V. Micol, N. Caturla, L. Perezfons, V. Mas, L. Perez, A. Estepa, The olive leaf extract exhibits antiviral activity against viral haemorrhagic septicaemia rhabdovirus (VHSV), *Antiviral Res.* 66 (2005) 129–136, <https://doi.org/10.1016/j.antiviral.2005.02.005>.
- [15] A.M. Dub, A.M. Dugani, Antithrombotic effect of repeated doses of the ethanolic extract of local olive (*Olea europaea* L.) leaves in rabbits, *Libyan J. Med.* 8 (2013) 20947, <https://doi.org/10.3402/ljm.v8i0.20947>.
- [16] D. Markin, L. Duek, I. Berdicevsky, In vitro antimicrobial activity of olive leaves. Antimikrobielle Wirksamkeit von Olivenblättern in vitro, *Mycoses* 46 (2003) 132–136, <https://doi.org/10.1046/j.1439-0507.2003.00859.x>.
- [17] H. Jemai, M. Bouaziz, I. Fki, A. El Fekki, S. Sayadi, Hypolipidemic and antioxidant activities of oleuropein and its hydrolysis derivative-rich extracts from Chemlali olive leaves, *Chem. Biol. Interact.* 176 (2008) 88–98, <https://doi.org/10.1016/j.cbi.2008.08.014>.
- [18] A. Saija, N. Uccella, Olive biophenols: functional effects on human wellbeing, *Trends Food Sci. Technol.* 11 (2000) 357–363, [https://doi.org/10.1016/S0924-2244\(00\)00068-6](https://doi.org/10.1016/S0924-2244(00)00068-6).
- [19] M.H. Elamin, M.H. Daghestani, S.A. Omer, M.A. Elobeid, P. Virk, E.M. Al-Olayan, Z.K. Hassan, O.B. Mohammed, A. Aboussekhra, Olive oil oleuropein has anti-breast cancer properties with higher efficiency on ER-negative cells, *Food Chem. Toxicol.* 53 (2013) 310–316, <https://doi.org/10.1016/j.fct.2012.12.009>.
- [20] S. Korkmaz, M. Sarimahmut, M.Z. Ozel, E. Ulukaya, Olive leaf extract containing oleuropein modulates the cytotoxic effect of epirubicin on breast cancer cells depending on the cell line, *Turk. J. Biochem.* 41 (2016), <https://doi.org/10.1515/tjb-2016-0117>.
- [21] L. Liu, K.S. Ahn, M.K. Shanmugam, H. Wang, H. Shen, F. Arfuso, A. Chinnathambi, S.A. Alharbi, Y. Chang, G. Sethi, F.R. Tang, Oleuropein induces apoptosis via abrogating NF- κ B activation cascade in estrogen receptor-negative breast cancer cells, *J. Cell. Biochem.* 120 (2019) 4504–4513, <https://doi.org/10.1002/jcb.27738>.
- [22] S. Fu, D. Arráez-Roman, A. Segura-Carretero, J.A. Menéndez, M.P. Menéndez-Gutiérrez, V. Micol, A. Fernández-Gutiérrez, Qualitative screening of phenolic compounds in olive leaf extracts by hyphenated liquid chromatography and preliminary evaluation of cytotoxic activity against human breast cancer cells, *Anal. Bioanal. Chem.* 397 (2010) 643–654, <https://doi.org/10.1007/s00216-010-3604-0>.
- [23] Z. Bouallagui, J. Han, H. Isoda, S. Sayadi, Hydroxytyrosol rich extract from olive leaves modulates cell cycle progression in MCF-7 human breast cancer cells, *Food Chem. Toxicol.* 49 (2011) 179–184, <https://doi.org/10.1016/j.fct.2010.10.014>.
- [24] E. Barrajón-Catalán, A. Taamalli, R. Quirantes-Piné, C. Roldán-Segura, D. Arráez-Román, A. Segura-Carretero, V. Micol, M. Zarrouk, Differential metabolomic analysis of the potential antiproliferative mechanism of olive leaf extract on the JIMT-1 breast cancer cell line, *J. Pharm. Biomed. Anal.* 105 (2015) 156–162, <https://doi.org/10.1016/j.jpba.2014.11.048>.
- [25] A. Di Francesco, A. Falconi, C. Di Germano, M.V. Micioni Di Bonaventura, A. Costa, S. Caramuta, M. Del Carlo, D. Compagnone, E. Dainese, C. Cifani, M. Maccarrone, C. D'Addario, Extravirgin olive oil up-regulates CB1 tumor suppressor gene in human colon cancer cells and in rat colon via epigenetic mechanisms, *J. Nutr. Biochem.* 26 (2015) 250–258, <https://doi.org/10.1016/j.jnutbio.2014.10.013>.
- [26] J. Ruzzolini, S. Peppicelli, F. Bianchini, E. Andreucci, S. Urciuoli, A. Romani, K. Tortora, G. Caderni, C. Nediani, L. Calorini, Cancer glycolytic dependence as a new target of olive leaf extract, *Cancers* 12 (2020) 317, <https://doi.org/10.3390/cancers12020317>.
- [27] D. Vizza, S. Lupinacci, G. Totada, F. Puoci, P. Ortensia I, A. De Bartolo, D. Lofaro, L. Scrivano, R. Bonofiglio, A. La Russa, M. Bonofiglio, A. Perri, An olive leaf extract rich in polyphenols promotes apoptosis in cervical cancer cells by upregulating p21^{Cip/WAF1} gene expression, *Nutr. Cancer* 71 (2019) 320–333, <https://doi.org/10.1080/01635581.2018.1559934>.
- [28] N.M. Ayoub, A.B. Siddique, H.Y. Ebrahim, M.M. Mohyeldin, K.A. El Sayed, The olive oil phenolic (-)-oleocanthal modulates estrogen receptor expression in luminal breast cancer in vitro and in vivo and synergizes with tamoxifen treatment, *Eur. J. Pharmacol.* 810 (2017) 100–111, <https://doi.org/10.1016/j.ejphar.2017.06.019>.
- [29] H. Rafehi, K. Ververis, T.C. Karagiannis, Mechanisms of action of phenolic compounds in olive, *J. Diet. Suppl.* 9 (2012) 96–109, <https://doi.org/10.3109/19390211.2012.682644>.
- [30] A.H. Stark, G. Kossoy, I. Zusman, G. Yarden, Z. Madar, Olive oil consumption during pregnancy and lactation in rats influences mammary cancer development in female offspring, *Nutr. Cancer* 46 (2003) 59–65, https://doi.org/10.1207/S15327914NC4601_08.
- [31] S. Ramos, Cancer chemoprevention and chemotherapy: dietary polyphenols and signalling pathways, *Mol. Nutr. Food Res.* 52 (2008) 507–526, <https://doi.org/10.1002/mnfr.200700326>.
- [32] L. Korkina, C. De Luca, V. Kostyuk, S. Pastore, Plant polyphenols and tumors: from mechanisms to therapies, prevention, and protection against toxicity of anti-cancer treatments, *CMC* 16 (2009) 3943–3965, <https://doi.org/10.2174/092986709789352312>.
- [33] A. Boss, K. Bishop, G. Marlow, M. Barnett, L. Ferguson, Evidence to support the anti-cancer effect of olive leaf extract and future directions, *Nutrients* 8 (2016) 513, <https://doi.org/10.3390/nu8080513>.
- [34] J. Ruzzolini, S. Peppicelli, E. Andreucci, F. Bianchini, A. Scardigli, A. Romani, G. la Marca, C. Nediani, L. Calorini, Oleuropein, the main polyphenol of *Olea europaea* leaf extract, has an anti-cancer effect on human BRAF melanoma cells and potentiates the cytotoxicity of current chemotherapies, *Nutrients* 10 (2018) 1950, <https://doi.org/10.3390/nu10121950>.
- [35] S.N. El, S. Karakaya, Olive tree (*Olea europaea*) leaves: potential beneficial effects on human health, *Nutr. Rev.* 67 (2009) 632–638, <https://doi.org/10.1111/j.1753-4887.2009.00248.x>.
- [36] M. de Bock, E.B. Thorstensen, J.G.B. Derraik, H.V. Henderson, P.L. Hofman, W. S. Cutfield, Human absorption and metabolism of oleuropein and hydroxytyrosol ingested as olive (*Olea europaea* L.) leaf extract, *Mol. Nutr. Food Res.* 57 (2013) 2079–2085, <https://doi.org/10.1002/mnfr.201200795>.
- [37] S. Mitra, R. Dash, Natural products for the management and prevention of breast cancer, *Evid. Based Complement. Altern. Med.* 2018 (2018) 1–23, <https://doi.org/10.1155/2018/8324696>.
- [38] A. Szarkowska, A. Kostecka, K. Meller, K.P. Bielawski, Inhibition of cancer antioxidant defense by natural compounds, *Oncotarget* 8 (2017), <https://doi.org/10.18632/oncotarget.13723>.
- [39] A.J. León-González, C. Auger, V.B. Schini-Kerth, Pro-oxidant activity of polyphenols and its implication on cancer chemoprevention and chemotherapy, *Biochem. Pharmacol.* 98 (2015) 371–380, <https://doi.org/10.1016/j.bcp.2015.07.017>.
- [40] S. D'Angelo, E. Martino, C.P. Ilisso, M.L. Bagarolo, M. Porcelli, G. Cacciapuoti, Pro-oxidant and pro-apoptotic activity of polyphenol extract from Annurca apple and its underlying mechanisms in human breast cancer cells, *Int. J. Oncol.* 51 (2017) 939–948, <https://doi.org/10.3892/ijo.2017.4088>.
- [41] S. Eghbaliferiz, M. Iranshahi, Prooxidant activity of polyphenols, flavonoids, anthocyanins and carotenoids: updated review of mechanisms and catalyzing metals: prooxidant activity of polyphenols and carotenoids, *Phytother. Res.* 30 (2016) 1379–1391, <https://doi.org/10.1002/ptr.5643>.
- [42] C.R. Reczek, N.S. Chandel, The two faces of reactive oxygen species in cancer, *Annu. Rev. Cancer Biol.* 1 (2017) 79–98, <https://doi.org/10.1146/annurev-cancerbio-041916-065808>.
- [43] E. Panieri, M.M. Santoro, ROS homeostasis and metabolism: a dangerous liaison in cancer cells, *Cell Death Dis.* 7 (2016) e2253, <https://doi.org/10.1038/cddis.2016.105>.
- [44] C. Goldsmith, D. Bond, H. Jankowski, J. Weidenhofer, C. Stathopoulos, P. Roach, C. Scarlett, The olive biophenols oleuropein and hydroxytyrosol selectively reduce proliferation, influence the cell cycle, and induce apoptosis in pancreatic Cancer cells, *IJMS* 19 (2018) 1937, <https://doi.org/10.3390/ijms19071937>.
- [45] Genetic/Familial high-risk assessment: breast and ovarian clinical practice guidelines, *J. Compr. Canc. Netw.* 4 (2006) 156, <https://doi.org/10.6004/jnccn.2006.0016>.
- [46] A.H. Eliassen, S.E. Hankinson, Endogenous hormone levels and risk of breast, endometrial and ovarian cancers: prospective studies, *Adv. Exp. Med. Biol.* 630 (2008) 148–165.
- [47] A. Antonosante, L. Brandolini, M. d'Angelo, E. Benedetti, V. Castelli, M.D. Maestro, S. Luzzi, A. Giordano, A. Cimini, M. Allegretti, Autocrine CXCL8-dependent invasiveness triggers modulation of actin cytoskeletal network and cell dynamics, *Aging* 12 (2020) 1928–1951, <https://doi.org/10.18632/aging.102733>.
- [48] D. Trisciuglio, M. Desideri, V. Farini, T. De Luca, M. Di Martile, M.G. Tupone, A. Urbani, S. D'Aguzzo, D. Del Bufalo, Affinity purification-mass spectrometry analysis of bcl-2 interactome identified SLIRP as a novel interacting protein, *Cell Death Dis.* 7 (2016) e2090, <https://doi.org/10.1038/cddis.2015.357>.
- [49] M. Zafarullah, W.Q. Li, J. Sylvester, M. Ahmad, Molecular mechanisms of N-acetylcysteine actions, *Cell. Mol. Life Sci. (CMLS)*. 60 (2003) 6–20, <https://doi.org/10.1007/s000180300001>.
- [50] V. Sosa, T. Moliné, R. Somoza, R. Paciucci, H. Kondoh, M.E. Lleonart, Oxidative stress and cancer: an overview, *Ageing Res. Rev.* 12 (2013) 376–390, <https://doi.org/10.1016/j.arr.2012.10.004>.
- [51] S.S. Sabharwal, P.T. Schumacker, Mitochondrial ROS in cancer: initiators, amplifiers or an Achilles' heel? *Nat. Rev. Cancer* 14 (2014) 709–721, <https://doi.org/10.1038/nrc3803>.
- [52] A. Yoneda, M.E. Lendorf, J.R. Couchman, H.A.B. Mulhaupt, Breast and ovarian cancers: a survey and possible roles for the cell surface heparan sulfate proteoglycans, *J. Histochem. Cytochem.* 60 (2012) 9–21, <https://doi.org/10.1369/0022155411428469>.
- [53] B. Corominas-Faja, R. Quirantes-Piné, C. Oliveras-Ferraro, A. Vazquez-Martin, S. Cufí, B. Martín-Castillo, V. Micol, J. Joven, A. Segura-Carretero, J.A. Menéndez, Metabolomic fingerprint reveals that metformin impairs one-carbon metabolism in a manner similar to the antifolate class of chemotherapy drugs, *Aging* 4 (2012) 480–498, <https://doi.org/10.18632/aging.100472>.
- [54] T.-I. Lafka, A. Lazou, V. Sinanoglou, E. Lazos, Phenolic extracts from wild olive leaves and their potential as edible oils antioxidants, *Foods* 2 (2013) 18–31, <https://doi.org/10.3390/foods2010018>.
- [55] A. Bendini, L. Cerretani, A. Carrasco-Pancorbo, A. Gómez-Caravaca, A. Segura-Carretero, A. Fernández-Gutiérrez, G. Lercker, Phenolic molecules in virgin olive oils: a survey of their sensory properties, health effects, antioxidant activity and analytical methods. An Overview of the Last Decade Alessandra, *Molecules* 12 (2007) 1679–1719, <https://doi.org/10.3390/12081679>.
- [56] S. Marino, C. Festa, F. Zollo, A. Nini, L. Antenucci, G. Raimo, M. Iorizzi, Antioxidant activity and chemical components as potential anticancer agents in the

- olive leaf (*Olea Europaea* L. Cv Leccino.) decoction, *ACAMC* 14 (2014) 1376–1385, <https://doi.org/10.2174/1871520614666140804153936>.
- [57] L. Vanella, Antiproliferative effect of oleuropein in prostate cell lines, *Int. J. Oncol.* (2012), <https://doi.org/10.3892/ijo.2012.1428>.
- [58] V. Kuete, A.T. Mbaveng, E.C.N. Nono, C.C. Simo, M. Zeino, A.E. Nkengfack, T. Efferth, Cytotoxicity of seven naturally occurring phenolic compounds towards multi-factorial drug-resistant cancer cells, *Phytomedicine*. 23 (2016) 856–863, <https://doi.org/10.1016/j.phymed.2016.04.007>.
- [59] V. Kuete, L.P. Sandjo, D.E. Djeussi, M. Zeino, G.M.N. Kwamou, B. Ngadjui, T. Efferth, Cytotoxic flavonoids and isoflavonoids from *Erythrina sigmoidea* towards multi-factorial drug resistant cancer cells, *Invest. New Drugs* 32 (2014) 1053–1062, <https://doi.org/10.1007/s10637-014-0137-y>.
- [60] X. Zhang, X. Wang, T. Wu, B. Li, T. Liu, R. Wang, Q. Liu, Z. Liu, Y. Gong, C. Shao, Isoliquinoline induces apoptosis in triple-negative human breast cancer cells through ROS generation and p38 MAPK/JNK activation, *Sci. Rep.* 5 (2015) 12579, <https://doi.org/10.1038/srep12579>.
- [61] P. Yu, C. Zhang, C.-Y. Gao, T. Ma, H. Zhang, M.-M. Zhou, Y.-W. Yang, L. Yang, L.-Y. Kong, Anti-proliferation of triple-negative breast cancer cells with physagulide P: ROS/JNK signaling pathway induces apoptosis and autophagic cell death, *Oncotarget* 8 (2017), <https://doi.org/10.18632/oncotarget.19299>.
- [62] X. Zhu, K. Wang, K. Zhang, L. Zhu, F. Zhou, Ziyuglycoside II induces cell cycle arrest and apoptosis through activation of ROS/JNK pathway in human breast cancer cells, *Toxicol. Lett.* 227 (2014) 65–73, <https://doi.org/10.1016/j.toxlet.2014.03.015>.
- [63] A. Nasimian, P. Farzaneh, F. Tamanoi, S.Z. Bathaie, Cytosolic and mitochondrial ROS production resulted in apoptosis induction in breast cancer cells treated with Crocin: The role of FOXO3a, PTEN and AKT signaling, *Biochem. Pharmacol.* 177 (2020) 113999, <https://doi.org/10.1016/j.bcp.2020.113999>.
- [64] E. Martino, D.C. Vuoso, S. D'Angelo, L. Mele, N. D'Onofrio, M. Porcelli, G. Cacciapuoti, Annurca apple polyphenol extract selectively kills MDA-MB-231 cells through ROS generation, sustained JNK activation and cell growth and survival inhibition, *Sci. Rep.* 9 (2019) 13045, <https://doi.org/10.1038/s41598-019-49631-x>.
- [65] C. Goldsmith, Q. Vuong, E. Sadeqzadeh, C. Stathopoulos, P. Roach, C. Scarlett, Phytochemical properties and anti-proliferative activity of *Olea europaea* L. Leaf extracts against pancreatic cancer cells, *Molecules* 20 (2015) 12992–13004, <https://doi.org/10.3390/molecules200712992>.
- [66] I. Samet, J. Han, L. Jlaïel, S. Sayadi, H. Isoda, Olive (*Olea europaea*) leaf extract induces apoptosis and Monocyte/Macrophage differentiation in human chronic myelogenous leukemia K562 cells: insight into the underlying mechanism, *Oxid. Med. Cell. Longev.* 2014 (2014) 1–16, <https://doi.org/10.1155/2014/927619>.
- [67] Y.-I. Yang, J.-H. Kim, K.-T. Lee, J.-H. Choi, Costunolide induces apoptosis in platinum-resistant human ovarian cancer cells by generating reactive oxygen species, *Gynecol. Oncol.* 123 (2011) 588–596, <https://doi.org/10.1016/j.ygyno.2011.08.031>.
- [68] J. Sánchez-Carranza, J. Díaz, M. Redondo-Horcajo, I. Barasoain, L. Alvarez, P. Lastres, A. Romero-Estrada, P. Aller, L. González-Maya, Gallic acid sensitizes paclitaxel-resistant human ovarian carcinoma cells through an increase in reactive oxygen species and subsequent downregulation of ERK activation, *Oncol. Rep.* (2018), <https://doi.org/10.3892/or.2018.6382>.
- [69] J.P. Alao, The regulation of cyclin D1 degradation: roles in cancer development and the potential for therapeutic invention, *Mol. Cancer* 6 (2007) 24, <https://doi.org/10.1186/1476-4598-6-24>.
- [70] C. Oleaga, C.J. Ciudad, V. Noé, M. Izquierdo-Pulido, Coffee polyphenols change the expression of stat5b and atf-2 modifying cyclin D1 levels in cancer cells, *Oxid. Med. Cell. Longev.* 2012 (2012) 1–17, <https://doi.org/10.1155/2012/390385>.
- [71] E. Shubbar, A. Kovács, S. Hajizadeh, T.Z. Parris, S. Nemes, K. Gunnarsdóttir, Z. Einbeigi, P. Karlsson, K. Helou, Elevated cyclin B2 expression in invasive breast carcinoma is associated with unfavorable clinical outcome, *BMC Cancer* 13 (2013) 1, <https://doi.org/10.1186/1471-2407-13-1>.
- [72] Y. Zhang, Y. Jiang, J. Wang, J. Ma, S. Han, Evaluation of core serous epithelial ovarian cancer genes as potential prognostic markers and indicators of the underlying molecular mechanisms using an integrated bioinformatics analysis, *Oncol. Lett.* (2019), <https://doi.org/10.3892/ol.2019.10884>.
- [73] M.R. Ramsey, N.E. Sharpless, ROS as a tumour suppressor? *Nat. Cell Biol.* 8 (2006) 1213–1215, <https://doi.org/10.1038/ncb1106-1213>.
- [74] M. Sciacovelli, E. Gaude, M. Hilvo, C. Frezza, The metabolic alterations of cancer cells. *Methods in Enzymology*, Elsevier, 2014, pp. 1–23, <https://doi.org/10.1016/B978-0-12-416618-9.00001-7>.
- [75] S. Vyas, E. Zaganjor, M.C. Haigis, Mitochondria and cancer, *Cell* 166 (2016) 555–566, <https://doi.org/10.1016/j.cell.2016.07.002>.
- [76] I. Vega-Naredo, R. Loureiro, K.A. Mesquita, I.A. Barbosa, L.C. Tavares, A.F. Branco, J.R. Erickson, J. Holy, E.L. Perkins, R.A. Carvalho, P.J. Oliveira, Mitochondrial metabolism directs stemness and differentiation in P19 embryonal carcinoma stem cells, *Cell Death Differ.* 21 (2014) 1560–1574, <https://doi.org/10.1038/cdd.2014.66>.
- [77] A. Wanet, T. Arnould, M. Najimi, P. Renard, Connecting mitochondria, metabolism, and stem cell fate, *Stem Cells Dev.* 24 (2015) 1957–1971, <https://doi.org/10.1089/scd.2015.0117>.
- [78] F. Guerra, A.A. Arbini, L. Moro, Mitochondria and cancer chemoresistance, *Biochim. et Biophys. Acta (BBA) - Bioenergetics* 1858 (2017) 686–699, <https://doi.org/10.1016/j.bbabi.2017.01.012>.
- [79] J. Neuzil, L.-F. Dong, J. Rohlena, J. Truksa, S.J. Ralph, Classification of mitocans, anti-cancer drugs acting on mitochondria, *Mitochondrion*. 13 (2013) 199–208, <https://doi.org/10.1016/j.mito.2012.07.112>.